AUTHOR QUERIES
AUTHOR PLEASE ANSWER ALL QUERIES

PLEASE NOTE: We cannot accept new source files as corrections for your paper. If possible, please annotate the PDF proof we have sent you with your corrections and upload it via the Author Gateway. Alternatively, you may send us your corrections in list format. You may also upload revised graphics via the Author Gateway.

If you have not completed your electronic copyright form (ECF) and payment option please return to the Scholar One "Transfer Center." In the Transfer Center you will click on "Manuscripts with Decisions" link. You will see your article details and under the "Actions" column click "Transfer Copyright." From the ECF it will direct you to the payment portal to select your payment options and then return to ECF for copyright submission.

AQ1: Author: Please confirm or add details for any funding or financial support for the research of this article.
AQ2: Please check the sentence "To visually illustrate the…" as only three components are listed here.
AQ3: Please provide the volume number and page range for Reference [11].
AQ4: Please provide the publisher location for Reference [29].
AQ5: Please provide the complete details and exact format for Reference [53].
AQ6: Please specify the field of the study for the Ph.D. degree of the author H. Chen.
AQ7: Please specify the field of study for the degrees attained by the authors R. Cheng and Y. Jin.

Solving Many-Objective Optimization Problems via Multistage Evolutionary Search

Huangke Chen, Ran Cheng, *Member, IEEE*, Witold Pedrycz, *Fellow, IEEE*, and Yaochu Jin, *Fellow, IEEE*

***Abstract*—With the increase in the number of optimization objectives, balancing the convergence and diversity in evolutionary multiobjective optimization becomes more intractable. So far, a variety of evolutionary algorithms have been proposed to solve many-objective optimization problems (MaOPs) with more than three objectives. Most of the existing algorithms, however, find difficulties in simultaneously counterpoising convergence and diversity during the whole evolutionary process. To address the issue, this paper proposes to solve MaOPs via multistage evolutionary search. To be specific, a two-stage evolutionary algorithm is developed, where the convergence and diversity are highlighted during different search stages to avoid the interferences between them. The first stage pushes multiple subpopulations with different weight vectors to converge to different areas of the Pareto front. After that the nondominated solutions coming from each subpopulation are selected for generating a new population for the second stage. Moreover, a new environmental selection strategy is designed for the second stage to balance the convergence and diversity close to the Pareto front. This selection strategy evenly divides each objective dimension into a number of intervals, and then one solution having the best convergence in each interval will be retained. To assess the performance of the proposed algorithm, 48 benchmark functions with 7, 10, and 15 objectives are used to make comparisons with five representative many-objective optimization algorithms.**

***Index Terms*—Evolutionary algorithm, many-objective optimization, multistage optimization.**

I. Introduction

REAL-WORLD optimization problems, such as parallel machine scheduling [1], hybrid electric vehicle optimization [2], and workflow scheduling in clouds [3], often need to simultaneously optimize multiple conflicting objectives, known as the multiobjective optimization problems (MOPs) [4], [5]

$$\begin{aligned} \text{Minimize} \quad & F(\mathbf{x}) = [f_1(\mathbf{x}), f_2(\mathbf{x}), \ldots, f_m(\mathbf{x})] \\ \text{s.t.} \quad & \mathbf{x} \in \Omega \end{aligned} \tag{1}$$

where $\mathbf{x} = (x_1, x_2, \ldots, x_n)$ represents the decision vector, and $\Omega \subseteq \mathbb{R}^n$ stands for the set of all the feasible decision vectors. The symbols n and m denote the number of decision variables and optimization objectives, respectively. The function $f_i(\mathbf{x})$ $\forall i \in \{1, 2, \ldots, m\}$ is used to map Ω to $\mathbb{R}$, i.e., $f_i : \Omega \to \mathbb{R}$. Specifically, an MOP with four or more objectives (i.e., $m \geq 4$) often refers to a many-objective optimization problem (MaOP) [6].

Due to the conflicts among the objectives of MOPs, improving one objective typically leads to the deterioration of the others [7]–[9]. Thus, there exists no single solution that can minimize all the objectives [10], [11], but a set of compromise solutions making tradeoffs among different objectives can be obtained. Regarding two solutions $\mathbf{x}_1, \mathbf{x}_2 \in \Omega$ of an MOP, $\mathbf{x}_1$ is considered to *dominate* $\mathbf{x}_2$ (expressed as $\mathbf{x}_1 \prec \mathbf{x}_2$) if $\mathbf{x}_1$ is better than or equal to $\mathbf{x}_2$ in all the objectives and $\mathbf{x}_1$ is strictly superior to $\mathbf{x}_2$ in at least one objective. One solution $\mathbf{x}^* \in \Omega$ is Pareto optimal if and only if there is no solution dominating it. In general, all the Pareto-optimal solutions comprise the Pareto optimal set, where the Pareto set (PS) and the Pareto-front (PF) are the images in the decision space and the objective space, respectively.

To obtain the Pareto optimal solutions for MOPs, a variety of multiobjective evolutionary algorithms (MOEAs) have been proposed over the past three decades [12], [13]. These existing algorithms are broadly divided into three categories: 1) Pareto dominance-based; 2) indicator-based; and 3) decomposition-based [12]. Pareto dominance-based MOEAs ~~are~~ often first sort the candidate solutions into many nondominated fronts, and then employ a secondary criterion to sort the solutions in the last accepted front. The classical works of this category

AQ1

Manuscript received October 19, 2018; revised March 23, 2019; accepted July 17, 2019. This work was supported in part by the National Key Research and Development Program of China under Grant 2017YFC0804002, in part by the Program for Guangdong Introducing Innovative and Entrepreneurial Teams under Grant 2017ZT07X386, in part by the Shenzhen Peacock Plan under Grant KQTD2016112514355531, in part by the Science and Technology Innovation Committee Foundation of Shenzhen under Grant ZDSYS201703031748284, and in part by the Program for University Key Laboratory of Guangdong Province under Grant 2017KSYS008. This paper was recommended by Associate Editor B. Derbel. *(Corresponding author: Ran Cheng.)*

H. Chen is with the College of Systems Engineering, National University of Defense Technology, Changsha 410073, China (e-mail: hkchen@nudt.edu.cn).

R. Cheng is with the Shenzhen Key Laboratory of Computational Intelligence, University Key Laboratory of Evolving Intelligent Systems of Guangdong Province, Department of Computer Science and Engineering, Southern University of Science and Technology, Shenzhen 518055, China (e-mail: ranchengcn@gmail.com).

W. Pedrycz is with the Department of Electrical and Computer Engineering, University of Alberta, Edmonton, AB T6G 2V4, Canada, also with the Department of Electrical and Computer Engineering, Faculty of Engineering, King Abdulaziz University, Jeddah 21589, Saudi Arabia, and also with the Systems Research Institute, Polish Academy of Sciences, 01447 Warsaw, Poland (e-mail: wpedrycz@ualberta.ca).

Y. Jin is with the Department of Computer Science, University of Surrey, Guildford GU2 7XH, U.K. (e-mail: yaochu.jin@surrey.ac.uk).

Color versions of one or more of the figures in this paper are available online at http://ieeexplore.ieee.org.

Digital Object Identifier 10.1109/TSMC.2019.2930737

are NSGA-II [14], MOPSO [15], etc. Regarding indicator-based MOEAs (e.g., HypE [16], AR-MOEA [17], BiGE [18], and others), a smaller number of indicators (e.g., one or two) related to the objective number are often used to sort the candidate solutions. For decomposition-based algorithms (e.g., MOEA/D and its variants [13], [19]–[21]), they partition the original MOP into many subproblems to be solved in a collaborative manner.

Although the existing MOEAs exhibit excellent performance in solving MOPs, their performance suffers from the curse of dimensionality with respect to the number of objectives in MaOPs, which can be attributed to three main reasons. First, the objective space of an MaOP expands exponentially with increasing number of objectives [22], [23], thus, resulting in a sparse distribution of the candidate solutions in the objective space, which poses a challenge to the diversity assessment [10]. Second, the increasing number of objectives leads to the dominance resistance [17], [24], [25], i.e., the percentage of nondominated candidate solutions in a population will sharply increase as the number of objectives, causing the failure of the dominance-based environmental selection strategies in MOEAs (e.g., NSGA-II, MOPSO, etc.) in distinguishing the candidate solutions. In addition, the PFs of MaOPs have various shapes, which will further challenge the tradeoffs between the convergence and the diversity. For example, some recent works have been demonstrated that the performance of the decomposition-based algorithms is greatly influenced by the PF shapes of MaOPs [17], [26].

To remedy the deficiency of MOEAs in solving the MaOPs, so far, a number of many-objective optimization algorithms (MaOEAs) have been reported [10], [12], [22], [27]. These MaOEAs typically follow the framework of MOEAs, mostly aiming to simultaneously strike a balance between convergence and diversity during the whole evolutionary process. However, as pointed in [10], despite that the convergence and diversity are two key factors to the performance of an MaOEA, they play different roles during different stages of the evolutionary process. Specifically, since the population of an MaOEA at the early search stage is still far from convergence, a higher convergence pressure is more desirable to push the population toward the PF. By contrast, at the later search stage, since the solutions are already near the PF, a wider spreading of the candidate solutions (i.e., diversity) is more preferable. Therefore, this motivates us to partition the whole evolutionary process into two stages, and the convergence is emphasized at the first stage, then the balance of convergence and diversity close to PF is emphasized at the second stage. This can avoid the negative effect of potential conflicts between the convergence and diversity. In summary, the key contributions of this paper are as follows.

1) A novel two-stage evolutionary algorithm, named TSEA, is proposed to partition the whole evolutionary search process into two stages. The first stage leverages multiple populations to accelerate the convergence toward the PF, followed by the balance of convergence and diversity at the second stage.
2) We design a novel environmental selection scheme for the second stage in TSEA to balance the convergence and diversity. This selection scheme evenly divides each objective dimension into a number of intervals and retains one candidate solution having the best convergence from each interval.
3) We conduct extensive experiments to compare the proposed TSEA with five representative algorithms on 48 test instances with various PF shapes, where the objective number ranges from 7 to 15. The experimental results demonstrate the superiorities of the proposed TSEA.

This paper is organized as follows. The recent works on MOEAs and MaOEAs are summarized in Section II. Then, the proposed TSEA is described in Section III, followed by extensive studies to verify and quantify the superiority of the TSEA. At last, Section V concludes this paper and provides a challenging direction.

II. Related Work

Over the past three decades, intensive attention has been given to the area of multiobjective evolutionary optimization, and a number of MOEAs have been developed and improved. Most existing MOEAs have focused on environmental selection strategies for balancing convergence and diversity. On the basis of the environmental selection strategies, the existing MOEAs are roughly grouped into the following three classes [12], [28]: 1) Pareto dominance-based; 2) indicator-based; and 3) decomposition-based.

For the Pareto dominance-based MOEAs, they first sort solutions into a series of nondominated levels ~~are~~ based on their dominance relationships, and then employ a secondary criterion to sort solutions in the last accepted level. The representative MOEAs of this category are the NSGA-II [14], PESA-II [29], MOPSO [15], and SPEA2 [30]. Besides, the Pareto dominance-based MOEAs have been widely used to solve various practical problems. For instance, Chen and Chou [31] modeled the crew roster recovery problems as multiobjective constrained combinational optimization problems and proposed a new version of the NSGA-II to search the Pareto solutions. To optimize the crude oil operations, Hou *et al.* [32] improved the NSGA-II using a new chromosome to model the feasible space. These algorithms show promising performance in solving problems having two or three objectives. Nevertheless, when increasing the number of objectives in MaOPs, the candidate solutions in a population often become incomparable with respect to their dominance relationships, which severely deteriorates their performances [25], [33]. To address the drawback of the Pareto dominance in distinguishing candidate solutions with many objectives, some new versions of Pareto dominance relation are designed, such as corner-sort-dominance [34], θ-dominance [33], grid-based dominance [35], fuzzy Pareto dominance [36], and alike. In addition, Chen *et al.* [37] proposed a hyperplane-assisted strategy to distinguish the nondominated solutions for many-objective optimization.

The indicator-based MOEAs often compare solutions using low-dimensional indicators (e.g., a single indicator [17] or two indicators [18]) instead of using their objective vectors directly. For instance, Zitzler and Künzli [38] defined a binary performance indicator to measure the solutions, and then designed a framework for indicator-based evolutionary algorithms. Beume *et al.* [39] combined the hypervolume indicator and the concept of nondominated sorting to form a selection strategy. However, the computation of the hypervolume indicator is time consuming when the number of objectives is large. To reduce the computational time of hypervolume, Bader and Zitzler [16] employed the Monte Carlo simulation for the hypervolume calculation. Bringmann *et al.* [40] empirically analyzed the performance impact of hypervolume-based Monte Carlo approximations on MOEAs, and concluded that the performance of MOEAs does not suffer from the inexact hypervolume. However, with the increasing number of objectives, the hypervolume calculation is still considerably expensive. Recently, Tian *et al.* [17] developed a new MOEA on the basis of an improved inverted generational distance indicator, and then designed a strategy to adaptively alter the reference vectors according to the indicator contributions of candidate solutions in the external archive. Zhou *et al.* [41] designed a co-guided MaOEA and used an indicator $_{\varepsilon+}I$ and reference points to improve the convergence and diversity. Li *et al.* [18] designed two indicators to, respectively, measure the convergence and diversity of the candidate solutions, and then employed the nondominated sorting method to balance the convergence and diversity based on these two indicators.

The decomposition-based MOEAs employ a set of weight vectors to decompose the MOP into a number of subproblems, which are solved in a collaborative way [13]. For instance, Zhang and Li [19] suggested the MOEA/D, which is among the most representative algorithms of this type. Wang *et al.* [42] suggested a preference-inspired algorithm to search interesting solutions for decision makers. Li *et al.* [43] combined the dominance-based strategy into the decomposition-based MOEAs to achieve good tradeoffs between the convergence and diversity. To adapt the MOEA/D to deal with the MOPs having complex PF shapes, Qi *et al.* [44] designed a strategy to adaptively adjust the weight vectors according to the geometric relationship between the weight vectors and the optimal solutions. Wang *et al.* [9] also proposed an adaptive adjustment strategy to adjust weight vectors for MOEA/D on the basis of the distribution of population located in the objective space. Wang *et al.* [45] demonstrated the importance of p-value in the L_p methods and designed a Pareto adaptive scalarizing strategy to find the near-optimal p-value. Cai *et al.* [46] suggested to use the angles between the objective vectors to improve the performance of MOEA/D in maintaining diversity. Cai *et al.* [47] proposed a constrained decomposition with grids to avoid the decomposition-based MOEAs being sensitive to the shapes of PFs. Elarbi *et al.* [48] designed a decomposition-based dominance relation and a diversity measurement for many-objective optimization. Wang *et al.* [49] used a localized weighted sum strategy to improve the performance decomposition-based MOEA in solving nonconvex problems.

A new direction of the decomposition-based approach is to divide the objective space of an MOP into many subspaces using a set of reference vectors, and then evolve the subpopulation belonging to each subspace cooperatively. The classical algorithms in this branch are the MOEA/D-M2M [20], MOEA/D-AM2M [50], and RVEA [10]. Chen *et al.* [51] proposed an indicator to measure the contribution of each subspace, and then designed an adaptive strategy to allocate computational resources for each subspace. To deal with the complicated PF shapes, Liu *et al.* [50] designed a new strategy to dynamically adjust the subregions of each subproblem on the basis of the obtained solutions. Kang *et al.* [52] improved the MOEA/D-M2M by designing a strategy to dynamically distribute computational resources to each subproblem according to their frequency of updating the external archive.

In summary, the aforementioned MOEAs strive to improve the population convergence and diversity simultaneously during the whole evolutionary process. However, emphasizing diversity during the early search stage will naturally weaken population convergence toward the PF, which is particularly serious when the PF has a complex shape. To address this issue, there also exist several works dedicated to solve MaOPs by multistage strategies. For instance, Cai *et al.* [53] improved the MOEA/D using a new strategy that first optimizes the boundary subproblems to obtain the corner solutions, then conducts the explorative search to extend the PF approximation. Hu *et al.* [54] designed a two-stage strategy to first obtain several extreme Pareto-optimal solutions, and then extend these obtained solutions to approximate the PF. In addition, Sun *et al.* [55] developed a two-stage strategy that strengthens the convergence at the first stage using an aggregation method, and then improves diversity using the decomposition-based approach. Similar to the above works, the proposed TSEA in this paper also partitions the whole evolutionary process into two stages. Different from these existing works, the first stage is proposed to push multiple subpopulations to different areas of the PF, and then at the second stage, a new environmental selection strategy is designed to balance convergence and diversity close to the PF.

So far, the angle-based methods have been widely used to measure the diversity of the candidate solutions. For example, the acute angles between solutions and reference vectors were used to associate solutions to different subspaces to maintain the population diversity [10], [20], [50]. Besides, the angles among solutions in objective space were utilized to measure the diversity of solutions [25], [56]. In the proposed TSEA, the angles between the solutions are also used as the diversity measurement. In addition, a new selection strategy is designed for TSEA to select solutions from each objective dimension, such that it can strike a good balance between convergence and diversity.

III. Two-Stage Evolutionary Algorithm

The proposed algorithm TSEA is detailed in this section. First, the main procedure of algorithm TSEA is given. Then, we describe the proposed two-stage evolutionary strategy. In the sequential, the novel environmental selection strategy is elaborated.

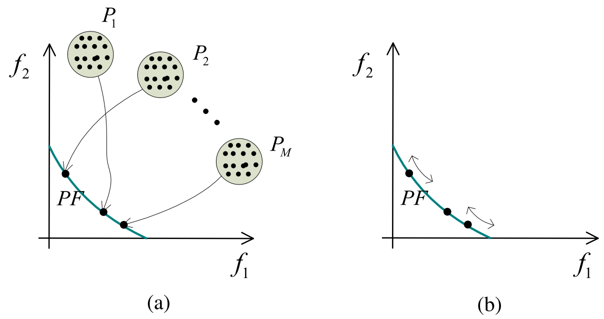

Fig. 1. Illustration of the proposed two-stage strategy. (a) At stage one, the subpopulations $P_1, P_2, \ldots, P_M$ are pushed close to the PF with respect to a set of weight vectors and (b) at stage two, the candidate solutions are diversified near the PF.

A. Main Procedure of TSEA

Before describing the proposed TSEA in detail, we provide a visual example in Fig. 1 to illustrate the main idea. The stage one of TSEA will randomly initialize a series of subpopulations, denoted by $P_1, P_2, \ldots, P_M$ in Fig. 1(a), and then pushes these subpopulations to different area of PF with respect to a set of weight vectors. After that the TSEA enters stage two to diversify the candidate solutions near the PF, which is shown in Fig. 1(b).

The framework of the algorithm TSEA is given in Algorithm 1. The main inputs of TSEA are: the optimization problem; the maximum number of function evaluations; the size of the output population; the number of subpopulations and the size of each subpopulation; and the convergence threshold Δ for subpopulations. Similar to other evolutionary algorithms [10], [22], the output of algorithm TSEA is the final population with N individuals.

As shown in Algorithm 1, the proposed TSEA first finds the diversity-related decision variables, and the set $\mathbf{I}_d$ is used to record all the diversity-related variables (line 1). Similar to [57] and [58], a decision variable is defined as diversity related if perturbing it only generates nondominated solutions. Then, M subpopulations with a size of N' are generated randomly (lines 3 and 4). To accelerate the convergence of each subpopulation toward the PF at the first stage, each subpopulation merely emphasizes the convergence, and we use different weight vectors to guide them toward different areas of the PF. Thus, an m-dimensional weight vector between 0 and 1 is randomly generated for each subpopulation (line 5). The arrays *bestF* and *conT* are used to record the best fitness and convergence status of each subpopulation (line 7). For each subpopulation, the well-known simulated binary crossover (SBX) and the polynomial mutation (PM) operators are applied to generate a new subpopulation (line 12). With respect to the subpopulation P_k, if the new solution in the new subpopulation Q_k has better fitness, it will replace the original solution in P_k (lines 13–15). The fitness of a solution p coming from subpopulation P_k is defined as $\mathrm{Fit}(p) = \sum_{i=1}^{m} W_{k,i} \cdot f_i$, where $W_{k,i}$ represents the ith element of weight vector W_k, and f_i denotes the ith objective value of solution p. Note that p_k^j and q_k^j represent the jth solution in P_k and Q_k, respectively (line 14). In addition, the best fitness of a subpopulation P_k

Algorithm 1: Main Procedure of the Proposed TSEA

Input: MaOP; maximal number of function evaluations (*MFEs*); population size N; number of subpopulations M; subpopulation size N'; threshold Δ;
Output: The final population A;

1 $\mathbf{I}_d \leftarrow$ Find the diversity-related variables;
2 Initialize the used function evaluations as $FEs \leftarrow 0$;
3 **for** $k = 1 \rightarrow M$ **do**
4   Initialize a subpopulation P_k with size N' randomly;
5   Randomly generate a m-dimensional vector W_k between 0 and 1;
6 $A \leftarrow \emptyset$;
7 $bestF_{1\times M} \leftarrow +\infty$; $conT_{1\times M} \leftarrow$ **FALSE**;
8 **while** $FEs < MFEs$ **do**
9   **for** $k = 1 \rightarrow M$ **do**
10   **if** $conT(k) == \boldsymbol{TRUE}$ **then**
11   **CONTINUE**;
12     $Q_k \leftarrow$ SBX+PM(P_k);
13   **for** $j = 1 \rightarrow N'$ **do**
14   **if** $Fit(p_k^j) \geq Fit(q_k^j)$ **then**
15         $p_k^j \leftarrow q_k^j$;
16   **if** $|bestFit(P_k) - bestF(k)| < \Delta$ **then**
17       $conT(k) \leftarrow$ **TRUE**;
18       $A \leftarrow A \bigcup P_k$;
19   Update A by removing dominated solutions;
20   **else**
21       $bestF(k) \leftarrow bestFit(P_k)$;
22   **if** *all the elements in conT are* ***TRUE*** **then**
23     $R \leftarrow$ Apply SBX and PM operator on $\mathbf{I}_d$ of A;
24     $A \leftarrow EnvironmentalSelection(A \bigcup R, N)$;

is denoted as bestFit(P_k), i.e., $\mathrm{bestFit}(P_k) = \min_{p \in P_k} \mathrm{Fit}(p)$. For a subpopulation, it is deemed to be converged in case the improvement of the best fitness among all the individuals is lower than the predetermined threshold Δ (line 16).

After all the subpopulations at the first stage have converged, all the nondominated solutions coming from the M subpopulations are selected to form a new population R (lines 18 and 19). Then, the algorithm enters the second stage (lines 22–24). During each iteration at this stage, a new population R is generated by applying SBX and PM operators on diversity-related variables $\mathbf{I}_d$ (line 23). Afterward, an environmental selection strategy is triggered to improve the population diversity (line 24), which is detailed in Algorithm 2.

B. Environmental Selection Approach

As shown in Algorithm 2, the proposed environmental selection strategy employs a three-step policy: 1) the first step is to remove dominated solutions from the combined population (line 1); 2) the second step evenly selects candidate solutions from each objective dimension (lines 2–16); and 3) the third step retains candidate solutions according to the cosine values

Algorithm 2: *EnvironmentalSelection*(Q, N)

Input: Combined population Q; size of population N;
Output: A selected population A;
1 Discard all the dominated solutions from Q;
2 $A \leftarrow \varnothing$; $S \leftarrow \varnothing$;
3 $T \leftarrow \lfloor \frac{N}{m} \rfloor$;
4 **for** $j = 1 \rightarrow m$ **do**
5 $\quad l \leftarrow$ The minimal value in the j-th objective of population Q;
6 $\quad u \leftarrow$ The maximal value in the j-th objective of population Q;
7 $\quad len \leftarrow \frac{u-l}{T-1}$;
8 $\quad$**for** $t = 1 \rightarrow T$ **do**
9 $\quad\quad I \leftarrow \varnothing$;
10 $\quad\quad$**for** $i = 1 \rightarrow |Q|$ **do**
11 $\quad\quad\quad$**if** $l + (t-1) \times len \leqslant F_{i,j} < l + t \times len$ **then**
12 $\quad\quad\quad\quad I \leftarrow I \bigcup \{i\}$;
13 $\quad\quad$**if** $I! = \varnothing$ & $I \bigcap S == \varnothing$ **then**
14 $\quad\quad\quad i \leftarrow$ Select the solution having the minimal sum of objective values among the set I;
15 $\quad\quad\quad S \leftarrow S \bigcup \{i\}$;
16 $\quad\quad\quad A \leftarrow A \bigcup Q(i)$;
17 $Q \leftarrow Q \setminus A$;
18 **while** $|P| < N$ & $Q! = \varnothing$ **do**
19 $\quad minCos \leftarrow 1$; $s \leftarrow 1$;
20 $\quad$**for** $i = 1 \rightarrow |Q|$ **do**
21 $\quad\quad maxCos \leftarrow 0$;
22 $\quad\quad$**for** $j = 1 \rightarrow |P|$ **do**
23 $\quad\quad\quad cos\theta_{i,j} \leftarrow$ Calculate the cosine between solution $Q(i)$ and $P(i)$;
24 $\quad\quad\quad$**if** $maxCos < cos\theta_{i,j}$ **then**
25 $\quad\quad\quad\quad maxCos \leftarrow cos\theta_{i,j}$;
26 $\quad\quad$**if** $maxCos < minCos$ **then**
27 $\quad\quad\quad minCos \leftarrow maxCos$; $s \leftarrow i$;
28 $\quad A \leftarrow A \bigcup Q(s)$;
29 $\quad Q \leftarrow Q \setminus Q(s)$;
30 Return the selected population A;

of the angles between the selected candidate solutions and the remaining ones (lines 17–29).

The set A, which is used to record the selected candidate solutions, is initialized as empty (line 2). Then, the set S is also initialized as empty (line 2), and it is used to record the indices of the selected solutions in the second step. Next, the number of solutions that are selected from each objective dimension is computed and denoted as T (line 3). Then, the objective values in each dimension are evenly divided into T intervals. For each interval, if there is no candidate solution selected in it (line 13), the one having the best convergence will be selected then (line 14), where the convergence is defined as the sum of its objective values. In addition, the symbol $F_{i,j}$ represents the value of the jth objective of the ith candidate solution in the population Q.

Afterward, all the selected candidate solutions are removed from Q (line 17), and the environmental selection strategy enters the third step, which will be iterated until the number of the selected candidate solutions $|P|$ reaching the population size N or the set Q becomes empty (line 18). During each iteration, the environmental selection strategy associates each remaining candidate solution with the maximal cosine value between it and all the selected candidate solutions (lines 21–25), and then selects the candidate solution having the minimal associated cosine value (lines 26 and 27). Next, the selected candidate solution will be added to the set A (line 28) and discarded from the set Q (line 29). Once the number of the selected candidate solutions reaches the population size or the set Q becomes empty, the third step will stop iterating and the selected population A will be returned (line 30).

IV. Experimental Studies

To quantitatively verify the effectiveness of the proposed TSEA, it is compared with five representative algorithms for many-objective optimization: 1) NSGA-III [22]; 2) RVEA [10]; 3) MaOEA-R&D [59]; 4) VaEA [25]; and 5) SPEA/R [27]. The five algorithms are briefly described as follows.

NSGA-III is the tailored version of the NSGA-II [14]. In *NSGA-III*, a new reference vector-based scheme is developed to strengthen the convergence when selecting candidate solutions in the last accepted front.

RVEA employs a set of reference vectors to divide the objective space of an MOP into a number of subspaces and associates each candidate solution with a reference vector having the minimal angle. Also, a new indicator, namely, angle penalized distance, is proposed to sort all the solutions in a subspace. Besides, the *RVEA* includes a strategy to adaptively adjust reference vectors according to the distribution of the candidate solutions.

MaOEA-R&D first searches for several solutions along m directions and construct the objective space boundary, and then adopts a diversity improvement strategy to improve the population diversity within the objective space boundary.

VaEA first employs the nondominated sorting approach to divide the candidate solutions into a number of fronts. For the solutions in the last accepted front, the solution having the largest acute angle to the selected solutions is iteratively selected until the number of selected solutions reaches the population size.

SPEA/R proposes a reference-based density assessment method and a fitness calculation method, then employs the diversity-first-and-convergence-second strategy to balance the convergence and diversity.

For these five algorithms in comparison, their source codes have been embedded into the PlatEMO,[1] which is an open-source MATLAB-based platform for multiobjective evolutionary optimization. The experiments in this paper follow the

[1]https://github.com/BIMK/PlatEMO

settings of these algorithms and problems in their published edition.

A. Experimental Settings

1) Benchmark Problems: To compare the performance of the six MOEAs, we utilize the following 16 benchmark functions: MaF1–MaF7 [60] and WFG1–WFG9 [57]. The benchmark functions MaF1–MaF7, which are specially designed for evaluating many-objective optimization, cover diverse properties, e.g., complicated Pareto front shapes, search landscapes, and alike. In addition, the nine benchmarks WFG1–WFG9 in the second test suite are widely used in the existing literature. In the experiments, a test instance refers to an MaOP with a specific number of objectives, e.g., benchmark WFG1 with seven objectives.

2) Performance Indicators: The hypervolume (HV) [61] and inverted generational distance (IGD) [62] are two widely used indicators to measure the effectiveness of MOEAs. The experimental studies in this paper also utilize them to compare the effectiveness of the six algorithms.

1) *HV:* It is defined as the volume of space, which consists of a reference point and all the output solutions in the objective space. The larger HV value means the better performance of the corresponding algorithm with respect to both the convergence and diversity. For each test instance, we set the reference point as 1.5 times of the upper bounds of its PF.
2) *IGD:* For an output population P, this metric is generally defined as

$$\mathrm{IGD}(P) = \frac{\sum_{v \in P^*} d(v, P)}{|P^*|} \tag{2}$$

where P^* stands for a set of sample Pareto optimal solutions on the PF, and $d(v, P)$ is the minimal distance between point v and all the points in P. Based on the definition in (2), a lower IGD value indicates the better performance of the corresponding algorithm. In our experiments, the P^* is set to contain around 8000 points for each test instance.

3) General Settings: For fair comparisons, the population sizes and termination conditions are set as follows.

1) *Population Size:* Similar to the existing works [10], [22], [25], [27], [59], the population size of the six algorithms is set according to the number of objectives of the test instances, i.e., 168, 230, and 240 for problems with 7, 10, and 15 objectives, respectively.
2) *Termination Condition:* For all the six algorithms, their termination conditions are set as the maximum number of function evaluations, i.e., 800 000 for MaF3 and MaF4; and 400 000 for the other benchmark functions.

B. Experimental Results

For statistical comparisons, the mean and standard deviation (in parentheses) of the HV and IGD values on all the test instances are summarized in Tables I and II, respectively. The Wilcoxon rank-sum test with $\alpha = 0.05$ is employed to verify the significant differences. The symbols $-$, $+$, and $\approx$ indicate that the indicator value of the corresponding algorithm has significantly worse, better, and similar performance in comparison with the proposed TSEA, respectively. For each test instance, the best HV and IGD values are highlighted.

The HV values of the six algorithms on the 16 benchmark functions with 7, 10, and 15 objectives are reported in Table I. From these experimental results, in summary, we can observe that the proposed TSEA shows generally the better performance in comparison with the other five algorithms with respect to the HV indicator. For the 48 test instances, TSEA significantly performs the best on 33 of them. To be specific, the TSEA outperforms *NSGA-III*, *RVEA*, *MaOEA-R&D*, *VaEA*, and *SPEA/R* on 43, 42, ~~48, and 36 of 34~~ test instances, respectively. Such better results illustrate the superiorities of the proposed TSEA with respect to both the convergence and diversity.

For the MaF test instances, except three test instances, namely, 7-objective MaF5, 10-objective MaF5, and 15-objective MaF7, the proposed TSEA generates significantly higher HV than the other algorithms on all the other test instances. For example, the HV value obtained by TSEA on 7-objective MaF1 on average is higher than algorithms *NSGA-III*, *RVEA*, *MaOEA-R&D*, *VaEA*, and *SPEA/R* by 74.06%, 358.42%, 1096.38%, 3.81%, and 371.97%, respectively. This is due to the fact that the stage one of TSEA only focuses on the population convergence and thus accelerates the convergence speed by avoiding the negative influence of the complicated PF shapes. By contrast, for the five algorithms in comparison, they employ the framework of traditional MOEAs to form tradeoffs between the population convergence and diversity simultaneously during the whole search process, which fails to work properly on problems with complicated PF shapes.

The WFG1–WFG9 benchmark functions are widely used to assess the effectiveness of MOEAs in solving many-objective problems. To further test the effectiveness of the algorithm TSEA, these 9 test functions with 7, 10, and 15 objectives are also used in the experimental comparisons. As shown in Table I, algorithm TSEA still significantly performs better than the five comparative algorithms on more than half of the test instances. Compared with *SPEA/R*, the proposed TSEA generates significantly higher HV values on 16 out of the 27 test instances. Regarding the *NSGA-III*, *RVEA*, *MaOEA-R&D*, and *VaEA*, the proposed TSEA performs better on even more instances.

For IGD indicator, the results of the six algorithms are summarized in Table II. Among the 48 test instances, the proposed TSEA generates significantly lower IGD values than *NSGA-III*, *RVEA*, *MaOEA-R&D*, *VaEA* and *SPEA/R* on 41, 39, 41, 27, and 35 test instances, respectively. In summary, TSEA outperforms the five compared algorithms on 25 out of the 48 test instances with respect to IGD indicator. These results again illustrate the promising performance of the algorithm TSEA.

To visually illustrate the distribution of the solution sets obtained by the six algorithms, we choose ~~four~~ test instances, AQ2 i.e., MaF1, MaF6, and WFG3 with ten objectives, to depict the objective vectors in parallel coordinates. For each algorithm, the solution sets with the lowest IGD value among 30 runs are shown in Figs. 2–4.

TABLE I
HV VALUES OF THE SIX ALGORITHMS ON BENCHMARK FUNCTIONS MaF1–MaF7 AND WFG1–WFG8 WITH 7, 10, AND 15 OBJECTIVES

MaOP	m	*NSGA-III*	*RVEA*	*MaOEA-R&D*	*VaEA*	*SPEA/R*	*TSEA*
MaF1	7	2.66e-1 (1.64e-2)−	1.01e-1 (2.76e-2)−	3.87e-2 (2.13e-3)−	4.46e-1 (4.29e-3)−	9.81e-2 (1.51e-2)−	4.63e-1 (3.98e-3)
	10	4.16e-2 (2.92e-3)−	1.06e-2 (1.87e-3)−	4.95e-3 (2.37e-4)−	1.02e-1 (2.39e-3)−	1.39e-2 (3.83e-3)−	1.07e-1 (2.46e-3)
	15	1.26e-3 (1.08e-4)−	2.85e-4 (6.01e-5)−	1.61e-4 (1.59e-5)−	5.06e-3 (1.72e-3)−	2.63e-4 (3.91e-5)−	5.62e-3 (1.09e-3)
MaF2	7	8.12e-1 (2.28e-2)−	6.94e-1 (5.36e-2)−	3.76e-1 (2.30e-2)−	8.95e-1 (7.29e-3)−	7.27e-1 (8.64e-2)−	9.23e-1 (3.62e-3)
	10	3.41e-1 (1.09e-2)−	2.68e-1 (4.79e-2)−	1.51e-1 (2.13e-2)−	3.46e-1 (2.60e-3)−	3.27e-1 (2.53e-3)−	3.60e-1 (1.76e-3)
	15	1.19e-2 (7.53e-4)−	7.57e-3 (3.79e-4)−	7.25e-3 (1.26e-3)−	1.15e-2 (1.08e-4)−	8.32e-3 (8.49e-4)−	1.55e-2 (1.07e-4)
MaF3	7	1.70e+1 (6.44e-3)−	1.70e+1 (2.41e-2)−	1.69e+1 (1.02e-1)−	1.56e+1 (1.49e+0)−	1.55e+1 (1.26e+0)−	1.71e+1 (1.91e-5)
	10	4.40e+1 (2.17e+1)−	5.76e+1 (4.29e-2)−	5.72e+1 (3.67e-1)−	5.70e+1 (1.05e+0)−	0.00e+0 (0.00e+0)−	5.77e+1 (3.6e-14)
	15	2.30e+2 (2.10e+2)−	4.37e+2 (1.07e-1)−	4.33e+2 (2.57e+0)−	1.50e+2 (1.90e+2)−	0.00e+0 (0.00e+0)−	4.38e+2 (1.2e-13)
MaF4	7	3.48e+8 (2.70e+7)−	6.30e+7 (1.10e+7)−	6.58e+7 (1.72e+7)−	4.54e+8 (1.87e+7)−	1.64e+8 (8.19e+7)−	4.76e+8 (6.76e+6)
	10	1.80e+16 (8e+14)−	1.15e+15 (4e+14)−	3.47e+15 (1e+15)−	2.45e+16 (1e+15)−	1.01e+16 (3e+15)−	2.59e+16 (6e+14)
	15	8.56e+34 (6e+33)−	9.35e+32 (1e+32)−	4.76e+34 (4e+34)−	1.02e+35 (1e+34)−	1.64e+34 (1e+34)−	1.13e+35 (7e+33)
MaF5	7	4.52e+9 (5.90e+5)≈	4.49e+9 (4.61e+7)−	4.33e+9 (4.51e+7)−	4.52e+9 (2.91e+6)≈	4.53e+9 (7.45e+5)+	4.52e+9 (1.31e+6)
	10	2.07e+18 (8e+13)≈	2.07e+18 (1e+15)≈	1.98e+18 (2e+16)−	2.07e+18 (4e+14)≈	2.07e+18 (1e+14)≈	2.07e+18 (1e+14)
	15	5.81e+38 (1e+35)−	5.81e+38 (2e+35)−	5.63e+38 (7e+36)−	5.81e+38 (1e+34)−	5.80e+38 (2e+34)−	5.82e+38 (4e+36)
MaF6	7	5.98e-3 (9.91e-5)−	5.76e-3 (6.34e-5)−	5.56e-3 (1.92e-7)−	6.03e-3 (1.15e-4)−	5.75e-3 (3.85e-5)−	6.05e-3 (7.61e-6)
	10	8.83e-7 (1.38e-6)−	3.76e-6 (1.37e-6)−	4.57e-6 (6.89e-9)−	4.40e-6 (1.57e-7)−	4.39e-6 (8.38e-7)−	4.78e-6 (6.89e-9)
	15	2.10e-15 (5e-15)−	3.25e-14 (9e-17)−	3.23e-14 (8e-17)−	3.08e-14 (1e-15)−	2.08e-15 (7e-15)−	3.30e-14 (5e-17)
MaF7	7	4.62e+1 (6.36e-1)−	4.38e+1 (5.93e-1)−	3.48e+1 (1.13e+0)−	4.67e+1 (2.40e-1)−	4.58e+1 (6.47e-1)−	4.73e+1 (2.78e-1)
	10	1.35e+2 (1.99e+0)−	1.13e+2 (2.28e+0)−	7.28e+1 (6.65e+0)−	1.35e+2 (1.12e+0)−	1.35e+2 (1.44e+0)−	1.38e+2 (7.48e-1)
	15	3.25e+2 (4.34e+1)−	1.94e+2 (9.85e+1)−	5.18e+1 (4.60e+1)−	6.56e+2 (4.77e+0)+	3.89e+2 (3.23e+2)−	6.49e+2 (2.20e+1)
WFG1	7	8.47e+6 (3.54e+5)−	8.93e+6 (5.11e+5)−	6.20e+6 (1.61e+6)−	1.05e+7 (2.67e+2)+	1.05e+7 (3.04e+1)+	9.71e+6 (6.07e+5)
	10	1.50e+11 (8.8e+9)−	1.84e+11 (9.5e+9)+	9.76e+10 (1e+10)−	1.92e+11 (8.9e+6)+	1.92e+11 (3.4e+5)+	1.74e+11 (1e+10)
	15	1.21e+19 (9e+17)−	1.40e+19 (6e+17)+	7.44e+18 (1e+18)−	1.46e+19 (3e+14)+	1.46e+19 (5e+13)+	1.32e+19 (1e+18)
WFG2	7	1.09e+7 (1.50e+4)−	1.08e+7 (4.13e+4)−	1.06e+7 (1.52e+5)−	1.09e+7 (6.06e+3)−	1.02e+7 (1.43e+3)−	1.10e+7 (5.23e+3)
	10	2.13e+11 (3.3e+8)−	2.11e+11 (7.3e+8)−	2.08e+11 (3.1e+9)−	2.13e+11 (1.4e+8)−	2.14e+11 (6.0e+7)−	2.15e+11 (1.2e+8)
	15	1.86e+19 (3e+16)−	1.83e+19 (1e+17)−	1.83e+19 (1e+17)−	1.87e+19 (1e+16)≈	1.87e+19 (1e+16)≈	1.87e+19 (7e+15)
WFG3	7	1.64e+0 (7.57e-1)−	2.50e-1 (4.98e-1)−	0.00e+0 (0.00e+0)−	3.45e+0 (3.02e-1)−	3.11e+0 (3.53e-1)−	4.68e+0 (1.44e-1)
	10	3.49e-5 (1.12e-4)−	0.00e+0 (0.00e+0)−	0.00e+0 (0.00e+0)−	3.11e-3 (4.35e-4)−	2.22e-3 (1.10e-3)−	4.09e-3 (6.09e-4)
	15	0.00e+0 (0.00e+0)−	0.00e+0 (0.00e+0)−	0.00e+0 (0.00e+0)−	0.00e+0 (0.00e+0)−	8.05e-16 (4e-15)−	9.27e-14 (6e-14)
WFG4	7	1.07e+7 (3.40e+4)−	1.06e+7 (4.01e+4)−	8.74e+6 (4.55e+5)−	1.08e+7 (7.29e+3)−	1.08e+7 (1.95e+3)−	1.09e+7 (7.10e+3)
	10	2.10e+11 (1.0e+9)−	2.09e+11 (6.7e+8)−	1.71e+11 (1e+10)−	2.12e+11 (2.1e+8)−	2.13e+11 (2.2e+7)−	2.14e+11 (2.2e+7)
	15	1.80e+19 (2e+17)−	1.82e+19 (9e+16)−	1.61e+19 (6e+17)−	1.86e+19 (2e+16)−	1.87e+19 (1e+16)−	1.88e+19 (5e+14)
WFG5	7	1.03e+7 (6.45e+3)−	1.04e+7 (6.84e+3)≈	8.19e+6 (2.66e+5)−	1.04e+7 (6.60e+3)≈	1.04e+7 (1.52e+3)≈	1.04e+7 (1.65e+5)
	10	2.03e+11 (1.1e+8)−	2.03e+11 (1.0e+8)−	1.49e+11 (9.5e+9)−	2.03e+11 (9.9e+7)−	2.03e+11 (8.1e+6)−	2.04e+11 (2.5e+7)
	15	1.74e+19 (1e+17)−	1.76e+19 (3e+16)−	1.41e+19 (1e+18)−	1.77e+19 (8e+15)−	1.77e+19 (3e+15)−	1.78e+19 (2e+16)
WFG6	7	1.01e+7 (1.31e+5)−	1.01e+7 (1.91e+5)−	7.71e+6 (5.17e+5)−	1.03e+7 (1.37e+5)−	1.03e+7 (1.32e+5)−	1.05e+7 (1.65e+5)
	10	1.98e+11 (3.8e+9)−	1.98e+11 (4.6e+9)−	1.49e+11 (1e+10)−	2.00e+11 (2.0e+9)−	2.04e+11 (2.9e+9)≈	2.04e+11 (5.0e+9)
	15	1.68e+19 (3e+17)−	1.69e+19 (4e+17)−	1.40e+19 (1e+18)−	1.75e+19 (2e+17)≈	1.75e+19 (2e+17)≈	1.75e+19 (5e+17)
WFG7	7	1.07e+7 (2.65e+4)−	1.07e+7 (2.84e+4)−	7.61e+6 (4.97e+5)−	1.08e+7 (3.99e+3)−	1.08e+7 (1.66e+3)−	1.09e+7 (2.56e+3)
	10	2.12e+11 (5.5e+8)−	2.12e+11 (3.7e+8)−	1.23e+11 (8.2e+9)−	2.13e+11 (3.3e+7)−	2.13e+11 (9.5e+6)−	2.14e+11 (1.5e+7)
	15	1.84e+19 (1e+17)−	1.79e+19 (3e+17)−	1.03e+19 (1e+18)−	1.87e+19 (1e+15)−	1.87e+19 (6e+15)−	1.88e+19 (4e+14)
WFG8	7	1.02e+7 (4.31e+4)−	9.55e+6 (4.25e+5)−	7.31e+6 (9.38e+5)−	1.03e+7 (3.35e+4)−	1.05e+7 (8.80e+4)+	1.04e+7 (6.92e+4)
	10	2.02e+11 (3.3e+9)−	1.83e+11 (1e+10)−	1.50e+11 (2e+10)−	2.07e+11 (6.0e+8)−	2.12e+11 (9.3e+8)+	2.09e+11 (2.1e+8)
	15	1.61e+19 (1e+18)−	1.53e+19 (1e+18)−	1.38e+19 (1e+18)−	1.84e+19 (6e+16)−	1.82e+19 (2e+17)−	1.86e+19 (6e+16)
WFG9	7	1.01e+7 (3.07e+5)≈	1.03e+7 (9.77e+4)+	7.54e+6 (3.89e+5)−	1.03e+7 (3.99e+5)+	1.04e+7 (1.24e+5)+	1.01e+7 (5.96e+5)
	10	1.97e+11 (9.5e+9)+	1.97e+11 (5.7e+9)+	1.39e+11 (1e+10)−	1.99e+11 (1e+10)+	2.07e+11 (1.0e+9)+	1.92e+11 (1e+10)
	15	1.77e+19 (7e+17)+	1.63e+19 (7e+17)−	1.249e+19 (1e+18)−	1.76e+19 (6e+17)+	1.76e+19 (2e+17)+	1.65e+19 (1e+18)

As shown in Fig. 2, the distribution of the output solution sets of the six algorithms is quite different. Fig. 2(a) shows that *NSGA-III* has good convergence and diversity in the first, second, third, and fifth objectives. For *RVEA*, the size of the solution set is much smaller than the predefined population size, referring to Fig. 2(b). The reason is that *RVEA* decomposes the objective space into a series of subspaces, and each subspace will retain at most one candidate solution. However, on the problems with complicated PF shapes, some subspaces may contain more than one representative candidate solutions, while some subspaces are completely empty. Except the sixth and seventh objectives, the convergence and diversity

TABLE II
IGD Values of the Six Algorithms on Benchmark Functions MaF1–MaF7 and WFG1–WFG8 With 7, 10, and 15 Objectives

MaOP	m	*NSGA-III*	*RVEA*	*MaOEA-R&D*	*VaEA*	*SPEA/R*	*TSEA*
MaF1	7	2.38e-1 (1.23e-2)−	4.95e-1 (7.87e-2)−	5.48e-1 (4.78e-2)−	1.81e-1 (8.45e-4)−	4.32e-1 (6.97e-2)−	1.79e-1 (1.50e-3)
	10	2.82e-1 (1.45e-2)−	5.73e-1 (9.08e-2)−	5.65e-1 (4.01e-2)−	2.41e-1 (1.69e-3)−	4.83e-1 (4.79e-2)−	2.40e-1 (2.18e-3)
	15	3.13e-1 (8.02e-3)−	6.40e-1 (7.20e-2)−	5.85e-1 (3.55e-2)−	2.78e-1 (1.12e-3)+	6.12e-1 (5.02e-2)−	3.02e-1 (3.74e-3)
MaF2	7	1.60e-1 (8.11e-3)−	2.31e-1 (7.29e-2)−	7.89e-1 (4.21e-2)−	1.48e-1 (3.35e-3)−	2.08e-1 (1.26e-1)−	1.47e-1 (2.64e-3)
	10	2.09e-1 (2.42e-2)−	4.52e-1 (2.10e-1)−	8.15e-1 (5.41e-2)−	1.86e-1 (3.29e-3)−	1.96e-1 (4.23e-4)−	1.85e-1 (3.14e-3)
	15	2.14e-1 (9.25e-3)−	4.95e-1 (1.43e-1)−	8.33e-1 (7.92e-2)−	2.04e-1 (2.13e-3)−	6.57e-1 (1.02e-1)−	1.98e-1 (2.25e-3)
MaF3	7	1.10e-1 (1.72e-2)−	9.27e-2 (4.36e-3)−	1.99e-1 (3.59e-2)−	2.88e-1 (9.34e-2)−	5.82e-1 (1.59e-1)−	7.56e-2 (6.42e-4)
	10	2.45e+0 (6.75e+0)−	8.29e-2 (9.59e-3)−	1.98e-1 (3.25e-2)−	1.95e-1 (2.86e-2)−	6.51e+4 (1.10e+5)−	6.95e-2 (4.80e-4)
	15	6.36e+1 (1.83e+2)	9.21e-2 (4.23e-3)−	2.12e-1 (3.37e-2)−	2.85e+0 (5.49e+0)−	2.15e+5 (3.05e+5)−	7.20e-2 (8.61e-5)
MaF4	7	1.30e+1 (1.12e+0)−	2.59e+1 (8.13e+0)−	6.16e+1 (5.19e+0)−	8.57e+0 (4.74e-1)−	2.33e+1 (6.05e+0)−	8.10e+0 (3.16e-1)
	10	9.58e+1 (8.05e+0)−	2.06e+2 (6.45e+1)−	5.22e+2 (4.72e+1)−	5.67e+1 (1.26e+1)−	1.35e+2 (3.21e+1)−	5.12e+1 (1.66e+0)
	15	3.75e+3 (2.43e+2)−	7.96e+3 (1.57e+3)−	1.49e+4 (4.11e+3)−	1.37e+3 (2.74e+2)−	5.23e+3 (1.03e+3)−	1.32e+3 (7.15e+1)
MaF5	7	9.21e+0 (5.02e-2)−	9.57e+0 (1.18e+0)−	8.91e+0 (2.85e+0)+	7.91e+0 (2.96e-1)+	9.25e+0 (3.05e-2)−	9.17e+0 (3.99e-1)
	10	8.70e+1 (1.38e+0)−	9.51e+1 (7.14e+0)−	5.47e+1 (1.33e+1)+	4.84e+1 (1.75e+0)+	8.80e+1 (1.71e+0)−	6.34e+1 (3.08e-2)
	15	2.39e+3 (2.78e+2)−	2.97e+3 (4.30e+2)−	1.56e+3 (5.86e+2)−	1.27e+3 (8.21e+1)+	2.26e+3 (2.27e+2)−	1.39e+3 (1.66e+2)
MaF6	7	3.01e-2 (3.43e-2)−	1.62e-1 (9.50e-2)−	7.42e-1 (6.59e-6)−	1.16e-2 (4.36e-2)−	9.87e-2 (2.23e-2)−	3.79e-3 (5.19e-5)
	10	7.43e+0 (2.41e+1)−	1.35e-1 (3.42e-2)−	7.37e-1 (1.74e-2)−	2.77e-1 (7.57e-2)−	2.21e-1 (1.12e-1)−	2.86e-3 (7.85e-7)
	15	8.91e+0 (9.65e+0)−	4.54e-1 (2.70e-1)−	7.09e-1 (4.55e-2)−	3.21e-1 (4.70e-2)−	3.61e+1 (3.49e+1)−	3.74e-3 (1.17e-6)
MaF7	7	6.03e-1 (5.53e-2)−	8.67e-1 (7.28e-2)−	1.28e+0 (1.62e-1)−	5.69e-1 (1.33e-2)≈	6.69e-1 (3.26e-2)−	5.69e-1 (1.82e-2)
	10	1.30e+0 (1.29e-1)−	1.90e+0 (3.98e-1)−	2.66e+0 (5.66e-1)−	9.55e-1 (1.82e-2)+	1.98e+0 (2.30e-2)−	9.75e-1 (1.52e-2)
	15	3.68e+0 (6.85e-1)−	2.70e+0 (5.10e-1)−	1.30e+1 (5.88e+0)−	1.97e+0 (1.10e-1)−	2.43e+1 (2.17e+1)−	1.80e+0 (2.41e-2)
WFG1	7	1.02e+0 (7.94e-2)−	9.53e-1 (1.06e-1)−	1.83e+0 (4.65e-1)−	7.68e-1 (4.58e-2)+	7.89e-1 (4.01e-2)+	8.21e-1 (5.80e-2)
	10	1.49e+0 (1.02e-1)−	1.52e+0 (1.39e-1)−	2.47e+0 (4.46e-1)−	1.13e+0 (6.54e-2)−	1.37e+0 (6.45e-2)−	1.22e+0 (6.86e-2)
	15	2.21e+0 (2.16e-1)−	1.98e+0 (1.35e-1)−	2.95e+0 (4.09e-1)−	1.80e+0 (7.94e-2)−	1.81e+0 (1.58e-1)−	1.79e+0 (1.21e-1)
WFG2	7	2.48e+0 (7.44e-1)−	5.40e+0 (1.02e+0)−	1.37e+0 (1.37e-1)+	2.22e+0 (2.62e-1)−	2.00e+0 (2.02e-1)+	2.08e+0 (2.14e-1)
	10	5.18e+0 (1.60e+0)−	7.54e+0 (2.12e+0)−	2.49e+0 (3.70e-1)+	2.87e+0 (2.69e-1)−	2.17e+0 (7.15e-1)+	2.41e+0 (1.82e-1)
	15	1.31e+1 (1.10e+0)−	1.85e+1 (4.84e+0)−	5.58e+0 (1.01e+0)−	1.02e+0 (3.66e-1)−	1.84e-1 (2.13e-1)−	5.11e-3 (1.52e-3)
WFG3	7	1.33e+0 (2.16e-1)−	1.52e+0 (2.54e-1)−	2.17e+0 (3.79e-1)−	1.08e+0 (1.62e-1)−	1.41e+0 (1.04e-1)−	2.55e-1 (1.13e-1)
	10	1.73e+0 (7.70e-1)−	4.15e+0 (6.89e-1)−	3.30e+0 (6.46e-1)−	1.83e+0 (1.99e-1)−	1.80e+0 (3.57e-2)−	5.15e-1 (2.88e-1)
	15	3.79e+0 (1.20e+0)−	8.07e+0 (2.04e+0)−	4.62e+0 (1.36e+0)−	3.65e+0 (1.81e-1)−	4.06e+0 (3.21e-1)−	1.14e+0 (6.99e-1)
WFG4	7	2.25e+0 (3.78e-2)+	2.22e+0 (6.07e-3)+	2.57e+0 (1.03e-1)+	2.27e+0 (1.84e-2)+	2.23e+0 (1.06e-3)+	2.64e+0 (2.63e-2)
	10	4.78e+0 (1.86e-1)+	4.59e+0 (6.08e-2)+	5.28e+0 (3.55e-1)+	4.19e+0 (2.80e-2)+	4.78e+0 (7.74e-3)+	4.82e+0 (3.60e-2)
	15	8.47e+0 (3.07e-1)−	8.87e+0 (1.30e-1)−	1.24e+1 (1.19e+0)−	7.43e+0 (7.94e-2)+	8.04e+0 (1.65e-2)+	8.05e+0 (7.10e-2)
WFG5	7	2.22e+0 (6.96e-3)−	2.21e+0 (4.79e-3)−	2.55e+0 (7.30e-2)−	2.26e+0 (1.52e-2)−	2.23e+0 (2.01e-4)−	2.19e+0 (1.07e-2)
	10	4.71e+0 (1.15e-2)+	4.59e+0 (6.86e-2)+	4.95e+0 (1.69e-1)−	4.18e+0 (2.84e-2)+	4.75e+0 (3.19e-3)+	4.78e+0 (3.36e-2)
	15	7.90e+0 (1.75e-1)+	8.80e+0 (1.13e-1)−	1.10e+1 (1.01e+0)−	7.18e+0 (5.79e-2)+	7.94e+0 (1.33e-2)+	7.95e+0 (6.43e-2)
WFG6	7	2.26e+0 (8.54e-3)+	2.24e+0 (2.91e-2)+	2.64e+0 (8.22e-2)−	2.29e+0 (2.20e-2)+	2.24e+0 (4.44e-3)+	2.63e+0 (2.56e-2)
	10	5.02e+0 (6.63e-1)−	4.43e+0 (9.06e-2)+	4.93e+0 (2.52e-1)−	4.25e+0 (3.68e-2)+	4.78e+0 (1.13e-2)+	4.82e+0 (3.78e-2)
	15	9.94e+0 (8.49e-1)−	9.23e+0 (3.47e-1)−	1.09e+1 (9.73e-1)−	7.23e+0 (5.58e-2)−	8.04e+0 (2.51e-2)−	7.19e+0 (4.64e-2)
WFG7	7	2.26e+0 (7.59e-3)−	2.21e+0 (7.28e-3)−	2.79e+0 (1.63e-1)−	2.26e+0 (1.93e-2)−	2.25e+0 (3.18e-3)−	2.20e+0 (8.51e-3)
	10	4.77e+0 (9.55e-2)−	4.57e+0 (3.67e-2)−	5.15e+0 (2.23e-1)−	4.17e+0 (2.11e-2)−	4.79e+0 (7.72e-3)−	4.05e+0 (2.12e-2)
	15	8.91e+0 (5.89e-1)−	7.72e+0 (5.34e-1)+	1.31e+1 (8.84e-1)−	7.21e+0 (4.84e-2)+	8.11e+0 (2.34e-2)−	7.98e+0 (4.55e-2)
WFG8	7	2.40e+0 (1.30e-1)−	2.41e+0 (3.92e-2)−	2.97e+0 (1.43e-1)−	2.43e+0 (2.72e-2)+	2.35e+0 (4.75e-2)+	2.67e+0 (4.56e-2)
	10	4.94e+0 (5.22e-1)−	4.36e+0 (6.93e-2)+	5.70e+0 (3.52e-1)+	4.45e+0 (3.86e-2)+	4.79e+0 (1.53e-2)−	4.74e+0 (5.49e-2)
	15	9.44e+0 (7.76e-1)−	8.91e+0 (3.76e-1)−	1.25e+1 (8.96e-1)−	7.37e+0 (2.50e-1)+	8.55e+0 (4.40e-2)−	8.15e+0 (1.21e-1)
WFG9	7	2.23e+0 (2.32e-2)+	2.20e+0 (7.97e-3)+	2.76e+0 (8.74e-2)−	2.23e+0 (1.92e-2)+	2.24e+0 (1.16e-2)+	2.60e+0 (2.31e-2)
	10	4.51e+0 (5.86e-2)+	4.48e+0 (6.77e-2)+	5.20e+0 (1.89e-1)−	4.13e+0 (2.47e-2)+	4.71e+0 (9.00e-3)+	4.72e+0 (7.25e-2)
	15	8.01e+0 (2.24e-1)−	7.69e+0 (2.72e-1)−	1.063e+1 (4.84e-1)−	6.93e+0 (5.23e-2)+	8.23e+0 (7.81e-2)−	7.68e+0 (1.05e-1)

of the output solution set obtained by *RVEA* are very poor. The complicated PF shape of MaF1 also weakens the convergence and diversity of *MaOEA-R&D* and *SPEA/R*, which is illustrated in Fig. 2(c) and (e). Fig. 2(d) shows that *VaEA* has better convergence and diversity than the other four comparison algorithms. By comparing Fig. 2(e) with Fig. 2(f), we can note that the distribution of the solution set obtained by the proposed TSEA is much better than *VaEA*. This also can explain why the HV and IGD values obtained by TSEA are much better than that obtained by the other five algorithms on the 10-objective MaF1, which are illustrated in the second row of Tables I and II.

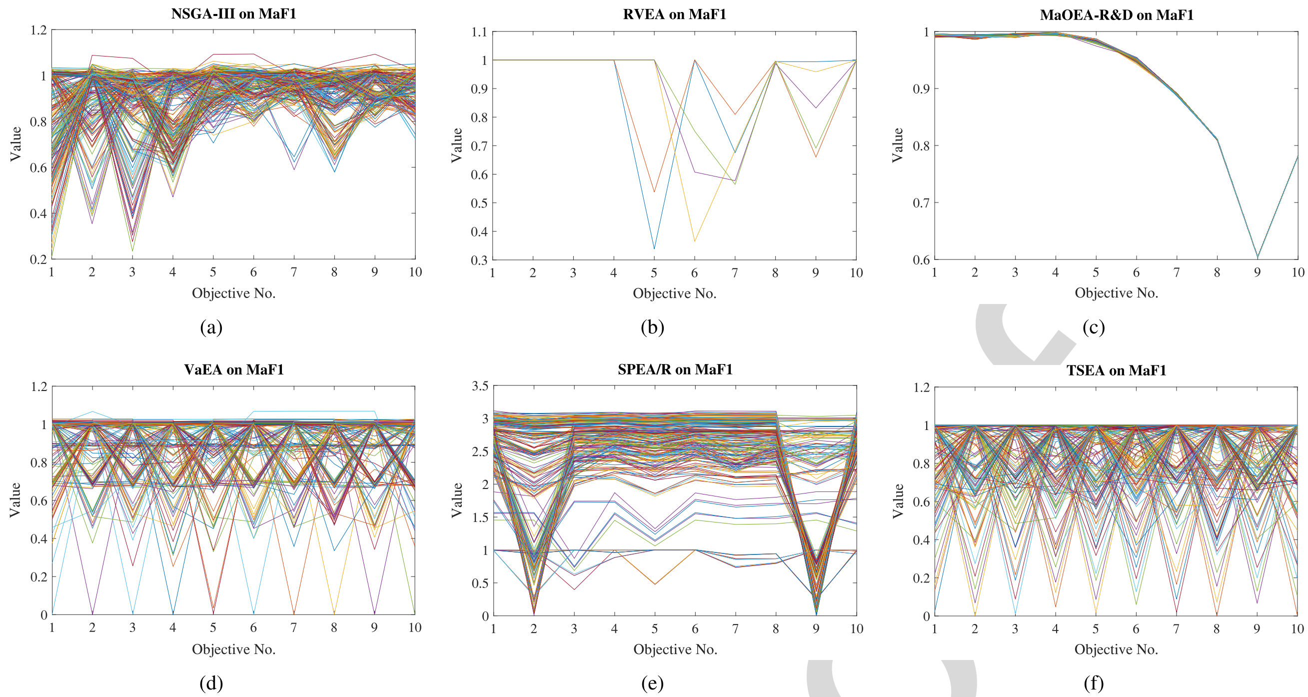

Fig. 2. Solution set obtained by each algorithm on the 10-objective MaF1, shown by parallel coordinates.

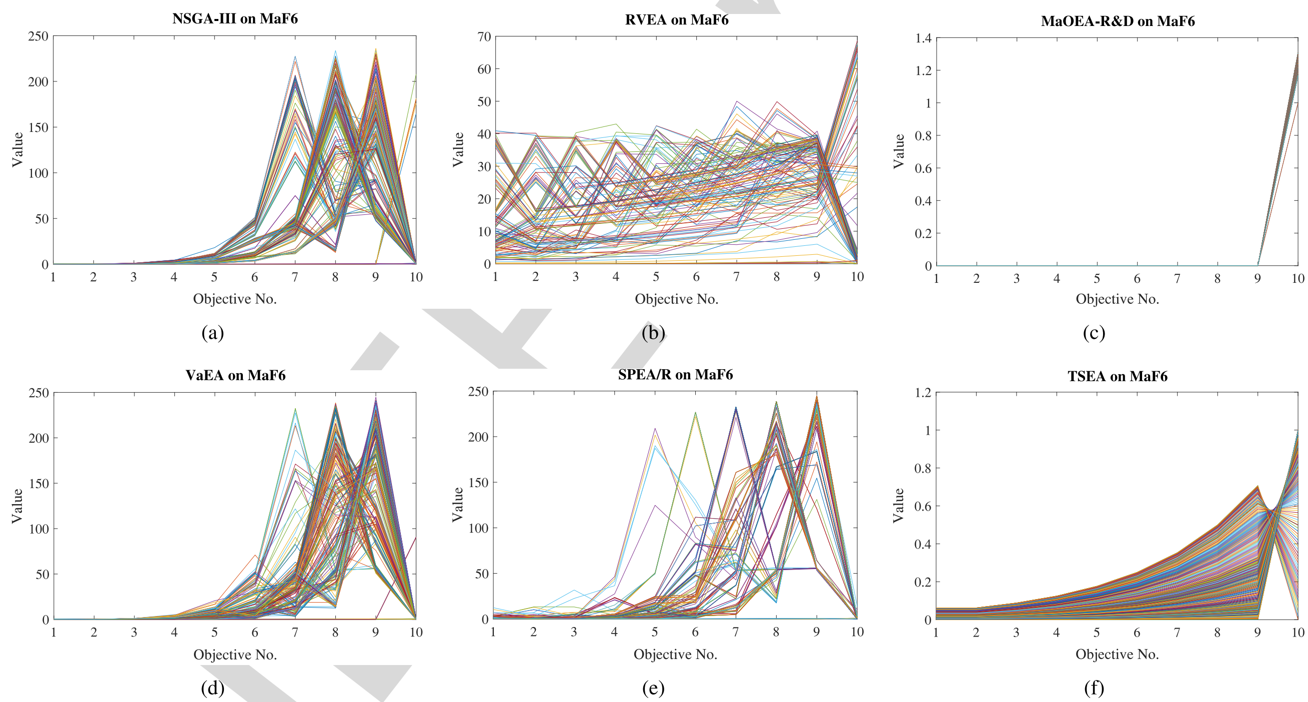

Fig. 3. Solution set obtained by each algorithm on the 10-objective MaF6, shown by parallel coordinates.

Since benchmark function MaF6 is a representative of MOPs with degenerate PFs, we also show the distribution of populations obtained by the six algorithms. As illustrated in Fig. 3, the convergence of *NSGA-III*, *RVEA*, *VaEA*, and *SPEA/R* is outperformed by the proposed TSEA. The algorithm *MaOEA-R&D* is similar to TSEA with respect to convergence, but the diversity of the proposed TSEA is better than that of *MaOEA-R&D*. This comparison results demonstrate the superiority of TSEA in solving MaOPs with disconnected PFs. In addition, the benchmark function WFG3 has also degenerate PF. For the test instance, i.e., 10-objective WFG3, it can be clearly observed that the proposed TSEA also outperforms the other five compared algorithms in terms of both convergence and diversity, which are illustrated in Fig. 4.

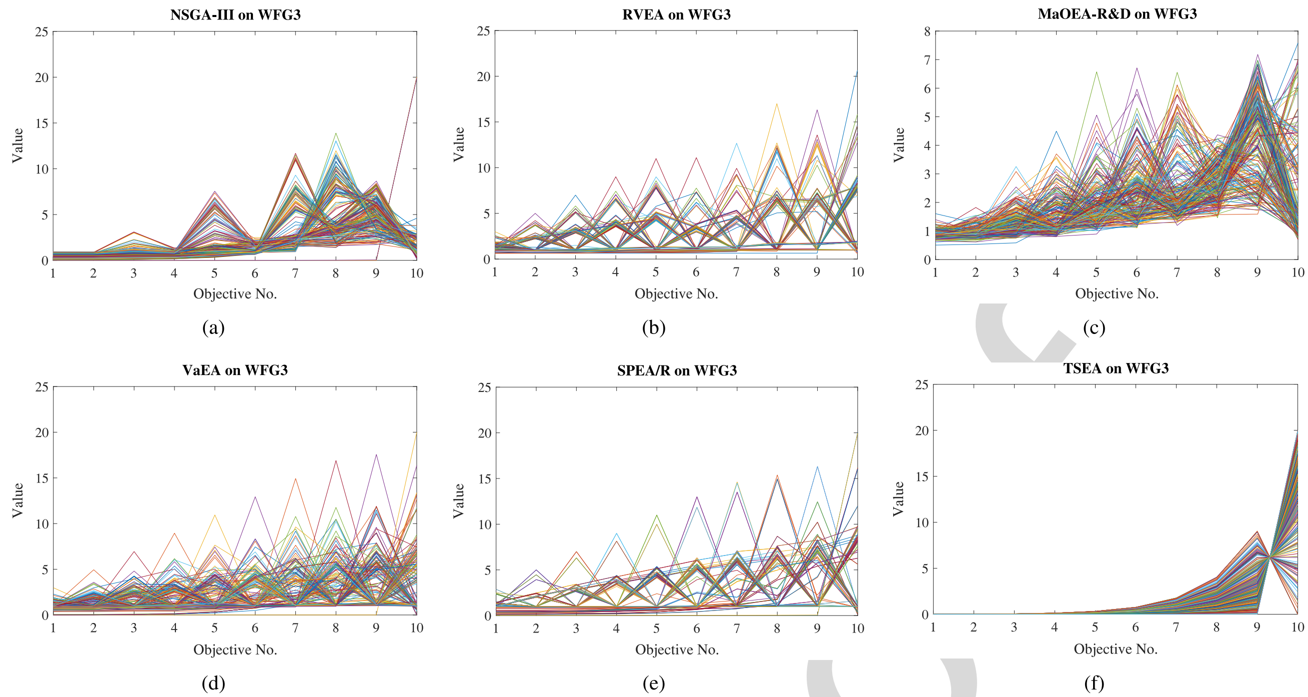

Fig. 4. Solution set obtained by each algorithm on the 10-objective WFG3, shown by parallel coordinates.

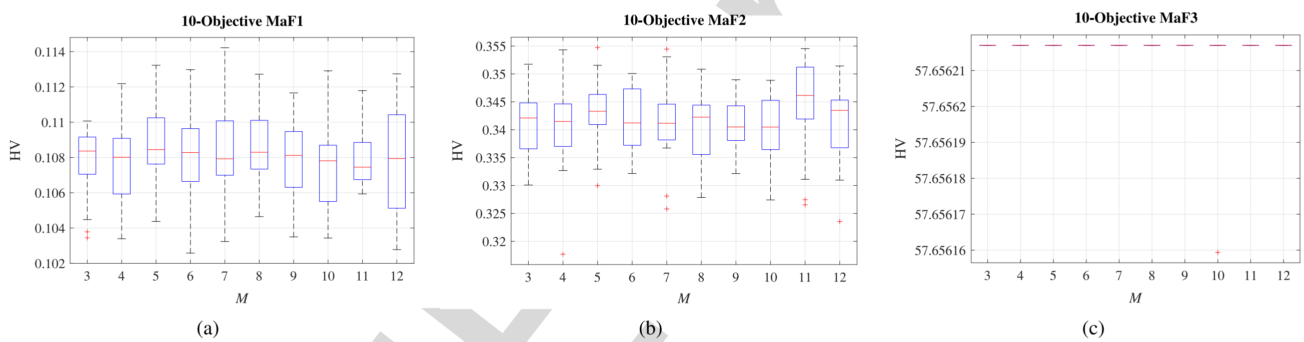

Fig. 5. Distributions of HV values obtained by TSEA over 30 runs by changing the parameter M.

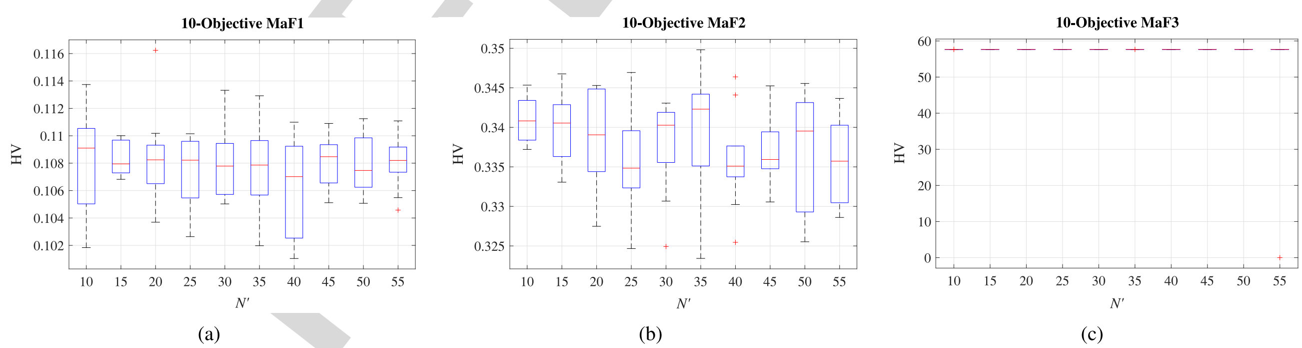

Fig. 6. Distributions of HV values obtained by TSEA over 30 runs by changing the parameter N'.

C. Sensitivity Analysis for Parameters M, N', and Δ

In the proposed TSEA, there are three tunable parameters: 1) the number of subpopulations M; 2) the size of a subpopulation N'; and 3) the convergence threshold Δ. To analyze the impact of these three parameters, in each experiment, we change the value of one parameter and fix the other two parameters. Besides, each experiment is repeated 30 times, and the box plots of the three parameters on 10-objective MaF1–MaF3 are illustrated in Figs. 5–7.

To test the impact of parameter M, it is varied from 3 to 12 with an increment of 1, while N' and Δ are fixed

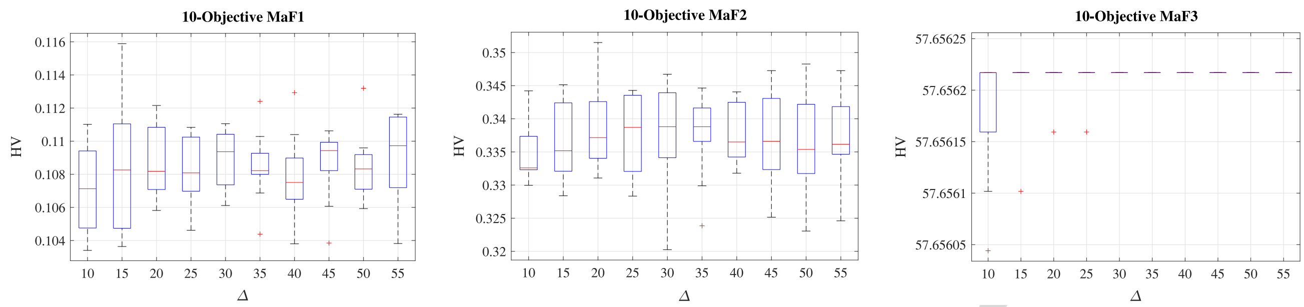

(a) (b) (c)

Fig. 7. Distributions of HV values obtained by TSEA over 30 runs by changing the parameter Δ.

to 20 and 1e-10, respectively. Fig. 5 shows that the HV values obtained by TSEA on the three test instances basically remain unchanged when varying parameter M. This result demonstrates that the parameter M has little impact on the performance of the proposed TSEA when it is between 3 and 12. A similar observation can be found in Fig. 6. When the size of each subpopulation is changed from 10 to 55, the HV values of TSEA on 10-objective MaF1, MaF2, and MaF3 are stable around 0.108, 0.336, and 57.656, respectively. This result illustrates that the parameter N' also has little impact on the performance of TSEA.

For parameter Δ, we change it from 1e-3 to 1e-12 to analyze its impact on the performance of the proposed TSEA. As shown in Fig. 7, we can see that the mean HV values obtained by TSEA on 10-objective MaF1 and MaF2 increase slightly with the decrease of parameter Δ. This can be attributed to the fact that lower Δ enables TSEA to push the subpopulations at the first stage closer to the PF, which is more helpful for balancing the convergence and diversity at the second stage. On the basis of the above analysis, we recommend the parameter Δ be lower than 1e–10 for the proposed TSEA.

V. Conclusion

This paper has proposed to solve MaOPs by partitioning the whole evolutionary search process into two stages, where the first stage focuses on the population convergence, and the second stage strives to improve the population diversity. To avoid the negative influence of the complicated PF shapes and accelerating the convergence speed of the population, all subpopulations at first stage only focuses on the convergence, and different weight vectors were used to guide them converge to different areas of PF. Then, to improve the population diversity, an environmental selection strategy has also proposed for the second stage to select the candidate solutions with promising diversity. Using such a multistage evolutionary search strategy, the proposed TSEA demonstrated ascendant performance over the five representative algorithms.

With the increase of the number of decision variables, the search spaces of optimization problems are exponentially ~~exploded~~, which seriously challenge the performance of evolutionary algorithms. Thus, solving MaOPs having thousands of decision variables is an interesting direction.

References

[1] X.-L. Zheng and L. Wang, "A collaborative multiobjective fruit fly optimization algorithm for the resource constrained unrelated parallel machine green scheduling problem," *IEEE Trans. Syst., Man, Cybern., Syst.*, vol. 48, no. 5, pp. 790–800, May 2018.

[2] R. Cheng, T. Rodemann, M. Fischer, M. Olhofer, and Y. Jin, "Evolutionary many-objective optimization of hybrid electric vehicle control: From general optimization to preference articulation," *IEEE Trans. Emerg. Topics Comput. Intell.*, vol. 1, no. 2, pp. 97–111, Apr. 2017.

[3] H. Chen, X. Zhu, G. Liu, and W. Pedrycz, "Uncertainty-aware online scheduling for real-time workflows in cloud service environment," *IEEE Trans. Services Comput.*, to be published. doi: 10.1109/TSC.2018.2866421.

[4] Z. Wang, Y.-S. Ong, J. Sun, A. Gupta, and Q. Zhang, "A generator for multiobjective test problems with difficult-to-approximate Pareto front boundaries," *IEEE Trans. Evol. Comput.*, to be published. doi: 10.1109/TEVC.2018.2872453.

[5] Y. R. Naidu and A. K. Ojha, "Solving multiobjective optimization problems using hybrid cooperative invasive weed optimization with multiple populations," *IEEE Trans. Syst., Man, Cybern., Syst.*, vol. 48, no. 6, pp. 821–832, Jun. 2018.

[6] M. Farina and P. Amato, "On the optimal solution definition for many-criteria optimization problems," in *Proc. IEEE Annu. Meeting North Amer. Fuzzy Inf. Process. Soc.*, 2002, pp. 233–238.

[7] L. Zhen, "A bi-objective model on multiperiod green supply chain network design," *IEEE Trans. Syst., Man, Cybern., Syst.*, to be published. doi: 10.1109/TSMC.2017.2690444.

[8] Z. Wang, Y.-S. Ong, and H. Ishibuchi, "On scalable multiobjective test problems with hardly-dominated boundaries," *IEEE Trans. Evol. Comput.*, vol. 23, no. 2, pp. 217–231, Apr. 2019.

[9] R. Wang, R. C. Purshouse, and P. J. Fleming, "Preference-inspired co-evolutionary algorithms using weight vectors," *Eur. J. Oper. Res.*, vol. 243, no. 2, pp. 423–441, 2015.

[10] R. Cheng, Y. Jin, M. Olhofer, and B. Sendhoff, "A reference vector guided evolutionary algorithm for many-objective optimization," *IEEE Trans. Evol. Comput.*, vol. 20, no. 5, pp. 773–791, Oct. 2016.

[11] H. Chen, R. Cheng, J. Wen, H. Li, and J. Weng, "Solving large-scale many-objective optimization problems by covariance matrix adaptation evolution strategy with scalable small subpopulations," *Inf. Sci.*, Oct. 2018. doi: 10.1016/j.ins.2018.10.007. AQ3

[12] B. Li, J. Li, K. Tang, and X. Yao, "Many-objective evolutionary algorithms: A survey," *ACM Comput. Surveys*, vol. 48, no. 1, pp. 1–35, 2015.

[13] A. Trivedi, D. Srinivasan, K. Sanyal, and A. Ghosh, "A survey of multiobjective evolutionary algorithms based on decomposition," *IEEE Trans. Evol. Comput.*, vol. 21, no. 3, pp. 440–462, Jun. 2017.

[14] K. Deb, A. Pratap, S. Agarwal, and T. Meyarivan, "A fast and elitist multiobjective genetic algorithm: NSGA-II," *IEEE Trans. Evol. Comput.*, vol. 6, no. 2, pp. 182–197, Apr. 2002.

[15] C. A. Coello Coello, G. T. Pulido, and M. S. Lechuga, "Handling multiple objectives with particle swarm optimization," *IEEE Trans. Evol. Comput.*, vol. 8, no. 3, pp. 256–279, Jun. 2004.

[16] J. Bader and E. Zitzler, "HypE: An algorithm for fast hypervolume-based many-objective optimization," *Evol. Comput.*, vol. 19, no. 1, pp. 45–76, Mar. 2011.

[17] Y. Tian, R. Cheng, X. Zhang, F. Cheng, and Y. Jin, "An indicator based multi-objective evolutionary algorithm with reference point adaptation for better versatility," *IEEE Trans. Evol. Comput.*, vol. 22, no. 4, pp. 609–622, Aug. 2018.

[18] M. Li, S. Yang, and X. Liu, "Bi-goal evolution for many-objective optimization problems," *Artif. Intell.*, vol. 228, pp. 45–65, Nov. 2015.

[19] Q. Zhang and H. Li, "MOEA/D: A multiobjective evolutionary algorithm based on decomposition," *IEEE Trans. Evol. Comput.*, vol. 11, no. 6, pp. 712–731, Dec. 2007.

[20] H.-L. Liu, F. Gu, and Q. Zhang, "Decomposition of a multiobjective optimization problem into a number of simple multiobjective subproblems," *IEEE Trans. Evol. Comput.*, vol. 18, no. 3, pp. 450–455, Jun. 2014.

[21] Z. Wang, Q. Zhang, A. Zhou, M. Gong, and L. Jiao, "Adaptive replacement strategies for MOEA/D," *IEEE Trans. Cybern.*, vol. 46, no. 2, pp. 474–486, Feb. 2016.

[22] K. Deb and H. Jain, "An evolutionary many-objective optimization algorithm using reference-point-based nondominated sorting approach, part I: Solving problems with box constraints," *IEEE Trans. Evol. Comput.*, vol. 18, no. 4, pp. 577–601, Aug. 2014.

[23] H. Ishibuchi, N. Akedo, and Y. Nojima, "Behavior of multiobjective evolutionary algorithms on many-objective knapsack problems," *IEEE Trans. Evol. Comput.*, vol. 19, no. 2, pp. 264–283, Apr. 2015.

[24] R. C. Purshouse and P. J. Fleming, "On the evolutionary optimization of many conflicting objectives," *IEEE Trans. Evol. Comput.*, vol. 11, no. 6, pp. 770–784, Dec. 2007.

[25] Y. Xiang, Y. Zhou, M. Li, and Z. Chen, "A vector angle-based evolutionary algorithm for unconstrained many-objective optimization," *IEEE Trans. Evol. Comput.*, vol. 21, no. 1, pp. 131–152, Feb. 2017.

[26] H. Ishibuchi, Y. Setoguchi, H. Masuda, and Y. Nojima, "Performance of decomposition-based many-objective algorithms strongly depends on Pareto front shapes," *IEEE Trans. Evol. Comput.*, vol. 21, no. 2, pp. 169–190, Apr. 2017.

[27] S. Jiang and S. Yang, "A strength Pareto evolutionary algorithm based on reference direction for multi-objective and many-objective optimization," *IEEE Trans. Evol. Comput.*, vol. 21, no. 3, pp. 329–346, Jun. 2017.

[28] A. Zhou, B.-Y. Qu, H. Li, S.-Z. Zhao, P. N. Suganthan, and Q. Zhang, "Multiobjective evolutionary algorithms: A survey of the state-of-the-art," *Swarm Evol. Comput.*, vol. 1, no. 1, pp. 32–49, 2011.

AQ4 [29] D. W. Corne, N. R. Jerram, J. D. Knowles, and M. J. Oates, "PESA-II: Region-based selection in evolutionary multiobjective optimization," in *Genetic and Evolutionary Computation*, Morgan Kaufmann, 2001, pp. 283–290.

[30] E. Zitzler, M. Laumanns, and L. Thiele, "SPEA2: Improving the strength Pareto evolutionary algorithm," in *Proc. Evol. Methods Design Optim. Control Appl. Ind. Problems*, 2002, pp. 95–100.

[31] C.-H. Chen and J.-H. Chou, "Multiobjective optimization of airline crew roster recovery problems under disruption conditions," *IEEE Trans. Syst., Man, Cybern., Syst.*, vol. 47, no. 1, pp. 133–144, Jan. 2017.

[32] Y. Hou, N. Wu, M. Zhou, and Z. Li, "Pareto-optimization for scheduling of crude oil operations in refinery via genetic algorithm," *IEEE Trans. Syst., Man, Cybern., Syst.*, vol. 47, no. 3, pp. 517–530, Mar. 2017.

[33] Y. Yuan, H. Xu, B. Wang, and X. Yao, "A new dominance relation-based evolutionary algorithm for many-objective optimization," *IEEE Trans. Evol. Comput.*, vol. 20, no. 1, pp. 16–37, Feb. 2016.

[34] H. Wang and X. Yao, "Corner sort for Pareto-based many-objective optimization," *IEEE Trans. Cybern.*, vol. 44, no. 1, pp. 92–102, Jan. 2014.

[35] S. Yang, M. Li, X. Liu, and J. Zheng, "A grid-based evolutionary algorithm for many-objective optimization," *IEEE Trans. Evol. Comput.*, vol. 17, no. 5, pp. 721–736, Oct. 2013.

[36] Z. He, G. G. Yen, and J. Zhang, "Fuzzy-based Pareto optimality for many-objective evolutionary algorithms," *IEEE Trans. Evol. Comput.*, vol. 18, no. 2, pp. 269–285, Apr. 2014.

[37] H. Chen, Y. Tian, W. Pedrycz, G. Wu, R. Wang, and L. Wang, "Hyperplane assisted evolutionary algorithm for many-objective optimization problems," *IEEE Trans. Cybern.*, to be published. doi: 10.1109/TCYB.2019.2899225.

[38] E. Zitzler and S. Künzli, "Indicator-based selection in multiobjective search," in *Proc. Parallel Problem Solving Nat.*, 2004, pp. 832–842.

[39] N. Beume, B. Naujoks, and M. Emmerich, "SMS-EMOA: Multiobjective selection based on dominated hypervolume," *Eur. J. Oper. Res.*, vol. 181, no. 3, pp. 1653–1669, 2007.

[40] K. Bringmann, T. Friedrich, C. Igel, and T. Voß, "Speeding up many-objective optimization by Monte Carlo approximations," *Artif. Intell.*, vol. 204, pp. 22–29, Nov. 2013.

[41] C. Zhou, G. Dai, M. Wang, and X. Li, "Indicator and reference points co-guided evolutionary algorithm for many-objective optimization problems," *Knowl. Based Syst.*, vol. 140, pp. 50–63, Jan. 2018.

[42] R. Wang, R. C. Purshouse, and P. J. Fleming, "Preference-inspired coevolutionary algorithms for many-objective optimization," *IEEE Trans. Evol. Comput.*, vol. 17, no. 4, pp. 474–494, Aug. 2013.

[43] K. Li, K. Deb, Q. Zhang, and S. Kwong, "An evolutionary many-objective optimization algorithm based on dominance and decomposition," *IEEE Trans. Evol. Comput.*, vol. 19, no. 5, pp. 694–716, Oct. 2015.

[44] Y. Qi, X. Ma, F. Liu, L. Jiao, J. Sun, and J. Wu, "MOEA/D with adaptive weight adjustment," *Evol. Comput.*, vol. 22, no. 2, pp. 231–264, 2014.

[45] R. Wang, Q. Zhang, and T. Zhang, "Decomposition-based algorithms using Pareto adaptive scalarizing methods," *IEEE Trans. Evol. Comput.*, vol. 20, no. 6, pp. 821–837, Dec. 2016.

[46] X. Cai, Z. Yang, Z. Fan, and Q. Zhang, "Decomposition-based-sorting and angle-based-selection for evolutionary multiobjective and many-objective optimization," *IEEE Trans. Cybern.*, vol. 47, no. 9, pp. 2824–2837, Sep. 2017.

[47] X. Cai, Z. Mei, Z. Fan, and Q. Zhang, "A constrained decomposition approach with grids for evolutionary multiobjective optimization," *IEEE Trans. Evol. Comput.*, vol. 22, no. 4, pp. 564–577, Aug. 2018.

[48] M. Elarbi, S. Bechikh, A. Gupta, L. B. Said, and Y.-S. Ong, "A new decomposition-based NSGA-II for many-objective optimization," *IEEE Trans. Syst., Man, Cybern., Syst.*, vol. 48, no. 7, pp. 1191–1210, Jul. 2018.

[49] R. Wang, Z. Zhou, H. Ishibuchi, T. Liao, and T. Zhang, "Localized weighted sum method for many-objective optimization," *IEEE Trans. Evol. Comput.*, vol. 22, no. 1, pp. 3–18, Feb. 2018.

[50] H.-L. Liu, L. Chen, Q. Zhang, and K. Deb, "Adaptively allocating search effort in challenging many-objective optimization problems," *IEEE Trans. Evol. Comput.*, vol. 22, no. 3, pp. 433–448, Jun. 2018.

[51] H. Chen, G. Wu, W. Pedrycz, P. N. Suganthan, L. Xing, and X. Zhu, "An adaptive resource allocation strategy for objective space partition based multiobjective optimization," *IEEE Trans. Syst., Man, Cybern., Syst.*, to be published. doi: 10.1109/TSMC.2019.2898456.

[52] Q. Kang, X. Song, M. Zhou, and L. Li, "A collaborative resource allocation strategy for decomposition-based multiobjective evolutionary algorithms," *IEEE Trans. Syst., Man, Cybern., Syst.*, to be published. doi: 10.1109/TSMC.2018.2818175.

[53] X. Cai, H. Sun, C. Zhu, Z. Li, and Q. Zhang, "Locating the boundaries of Pareto fronts: A many-objective evolutionary algorithm based on corner solution search," *arXiv preprint arXiv:1806.02967*, 2018. AQ5

[54] W. Hu, G. G. Yen, and G. Luo, "Many-objective particle swarm optimization using two-stage strategy and parallel cell coordinate system," *IEEE Trans. Cybern.*, vol. 47, no. 6, pp. 1446–1459, Jun. 2017.

[55] Y. Sun, B. Xue, M. Zhang, and G. G. Yen, "A new two-stage evolutionary algorithm for many-objective optimization," *IEEE Trans. Evol. Comput.*, to be published. doi: 10.1109/TEVC.2018.2882166.

[56] Y. Liu, D. Gong, J. Sun, and Y. Jin, "A many-objective evolutionary algorithm using a one-by-one selection strategy," *IEEE Trans. Cybern.*, vol. 47, no. 9, pp. 2689–2702, Sep. 2017.

[57] S. Huband, P. Hingston, L. Barone, and L. While, "A review of multiobjective test problems and a scalable test problem toolkit," *IEEE Trans. Evol. Comput.*, vol. 10, no. 5, pp. 477–506, Oct. 2006.

[58] X. Ma *et al.*, "A multiobjective evolutionary algorithm based on decision variable analyses for multiobjective optimization problems with large-scale variables," *IEEE Trans. Evol. Comput.*, vol. 20, no. 2, pp. 275–298, Apr. 2016.

[59] Z. He and G. G. Yen, "Many-objective evolutionary algorithm: Objective space reduction and diversity improvement," *IEEE Trans. Evol. Comput.*, vol. 20, no. 1, pp. 145–160, Feb. 2016.

[60] R. Cheng *et al.*, "A benchmark test suite for evolutionary many-objective optimization," *Complex Intell. Syst.*, vol. 3, no. 1, pp. 67–81, 2017.

[61] E. Zitzler and L. Thiele, "Multiobjective evolutionary algorithms: A comparative case study and the strength Pareto approach," *IEEE Trans. Evol. Comput.*, vol. 3, no. 4, pp. 257–271, Nov. 1999.

[62] P. A. N. Bosman and D. Thierens, "The balance between proximity and diversity in multiobjective evolutionary algorithms," *IEEE Trans. Evol. Comput.*, vol. 7, no. 2, pp. 174–188, Apr. 2003.

Huangke Chen received the B.S. degree in management science and engineering and the M.S. degree in operations research from the College of Information and System Management, National University of Defense Technology, Changsha, China, in 2012 and 2014, respectively, where he is currently pursuing the Ph.D. degree with the College of Systems Engineering.

He was a visiting Ph.D. student with the University of Alberta, Edmonton, AB, Canada, from 2017 to 2018. His current research interests include computational intelligence, multiobjective evolutionary algorithms, large-scale optimization, and task and workflow scheduling.

Ran Cheng (M'16) received the B.Sc. degree from Northeastern University, Shenyang, China, in 2010, and the Ph.D. degree from the University of Surrey, Guildford, U.K., in 2016.

He is currently an Assistant Professor with the Department of Computer Science and Engineering, Southern University of Science and Technology, Shenzhen, China. His current research interests include evolutionary multiobjective optimization, model-based evolutionary algorithms, large-scale optimization, swarm intelligence, and deep learning.

Dr. Cheng was a recipient of the 2018 IEEE TRANSACTIONS ON EVOLUTIONARY COMPUTATION Outstanding Paper Award, the 2019 IEEE Computational Intelligence Society Outstanding Ph.D. Dissertation Award, and the 2020 *IEEE Computational Intelligence Magazine* Outstanding Paper Award. He is the Founding Chair of IEEE Symposium on Model-Based Evolutionary Algorithms.

Witold Pedrycz (F'99) received the M.Sc., Ph.D., and D.Sc. degrees in computer science from the Silesian University of Technology, Gliwice, Poland.

He is a Professor and the Canada Research Chair of CRC-Computational Intelligence with the Department of Electrical and Computer Engineering, University of Alberta, Edmonton, AB, Canada, also with the Department of Electrical and Computer Engineering, Faculty of Engineering, King Abdulaziz University, Jeddah, Saudi Arabia, and also with the Systems Research Institute, Polish Academy of Sciences, Warsaw, Poland. His current research interests include computational intelligence, fuzzy modeling and granular computing, knowledge discovery and data mining, fuzzy control, pattern recognition, knowledge-based neural networks, relational computing, and software engineering. He has published numerous papers in the above areas.

Prof. Pedrycz is the Editor-in-Chief of *Information Sciences* and serves as an Associate Editor for the IEEE TRANSACTIONS ON SYSTEMS, MAN, AND CYBERNETICS: SYSTEMS and IEEE TRANSACTIONS ON FUZZY SYSTEMS. He is also on the editorial board of other international journals.

Yaochu Jin (M'98–SM'02–F'16) received the B.Sc., M.Sc., and Ph.D. degrees from Zhejiang University, Hangzhou, China, in 1988, 1991, and 1996, respectively, and the Dr.-Ing. degree from Ruhr University Bochum, Bochum, Germany, in 2001.

He is a Professor of Computational Intelligence with the Department of Computer Science, University of Surrey, Guildford, U.K., where he heads the Nature Inspired Computing and Engineering Group. He is also a Finland Distinguished Professor funded by the Finnish Agency for Innovation (Tekes) and a Changjiang Distinguished Visiting Professor appointed by the Ministry of Education, Beijing, China. He has coauthored over 200 peer-reviewed journal and conference papers and been granted eight patents on evolutionary optimization. His current research is funded by EC FP7, U.K. EPSRC, and industry. He has delivered over 20 invited keynote speeches at international conferences. His science-driven research interests include interdisciplinary areas that bridge the gap between computational intelligence, computational neuroscience, and computational systems biology. He is also particularly interested in nature-inspired and real-world-driven problem solving.

Prof. Jin was a recipient of the Best Paper Award of the 2010 IEEE Symposium on Computational Intelligence in Bioinformatics and Computational Biology and the 2014 and 2017 *IEEE Computational Intelligence Magazine* Outstanding Paper Award. He is the Editor-in-Chief of the IEEE TRANSACTIONS ON COGNITIVE AND DEVELOPMENTAL SYSTEMS and *Complex and Intelligent Systems*. He is also an Associate Editor or an Editorial Board Member of the IEEE TRANSACTIONS ON EVOLUTIONARY COMPUTATION, IEEE TRANSACTIONS ON CYBERNETICS, IEEE TRANSACTIONS ON NANOBIOSCIENCE, *Evolutionary Computation*, *BioSystems*, *Soft Computing*, and *Natural Computing*. He is an IEEE Distinguished Lecturer from 2013 to 2015 and from 2017 to 2019, and was the Vice President for Technical Activities of the IEEE Computational Intelligence Society from 2014 to 2015.

AUTHOR QUERIES

AUTHOR PLEASE ANSWER ALL QUERIES

PLEASE NOTE: We cannot accept new source files as corrections for your paper. If possible, please annotate the PDF proof we have sent you with your corrections and upload it via the Author Gateway. Alternatively, you may send us your corrections in list format. You may also upload revised graphics via the Author Gateway.

If you have not completed your electronic copyright form (ECF) and payment option please return to the Scholar One "Transfer Center." In the Transfer Center you will click on "Manuscripts with Decisions" link. You will see your article details and under the "Actions" column click "Transfer Copyright." From the ECF it will direct you to the payment portal to select your payment options and then return to ECF for copyright submission.

AQ1: Author: Please confirm or add details for any funding or financial support for the research of this article.

AQ2: Please check the sentence "To visually illustrate the…" as only three components are listed here.

AQ3: Please provide the volume number and page range for Reference [11].

AQ4: Please provide the publisher location for Reference [29].

AQ5: Please provide the complete details and exact format for Reference [53].

AQ6: Please specify the field of the study for the Ph.D. degree of the author H. Chen.

AQ7: Please specify the field of study for the degrees attained by the authors R. Cheng and Y. Jin.

Solving Many-Objective Optimization Problems via Multistage Evolutionary Search

Huangke Chen, Ran Cheng, *Member, IEEE*, Witold Pedrycz, *Fellow, IEEE*, and Yaochu Jin, *Fellow, IEEE*

***Abstract*—With the increase in the number of optimization objectives, balancing the convergence and diversity in evolutionary multiobjective optimization becomes more intractable. So far, a variety of evolutionary algorithms have been proposed to solve many-objective optimization problems (MaOPs) with more than three objectives. Most of the existing algorithms, however, find difficulties in simultaneously counterpoising convergence and diversity during the whole evolutionary process. To address the issue, this paper proposes to solve MaOPs via multistage evolutionary search. To be specific, a two-stage evolutionary algorithm is developed, where the convergence and diversity are highlighted during different search stages to avoid the interferences between them. The first stage pushes multiple subpopulations with different weight vectors to converge to different areas of the Pareto front. After that the nondominated solutions coming from each subpopulation are selected for generating a new population for the second stage. Moreover, a new environmental selection strategy is designed for the second stage to balance the convergence and diversity close to the Pareto front. This selection strategy evenly divides each objective dimension into a number of intervals, and then one solution having the best convergence in each interval will be retained. To assess the performance of the proposed algorithm, 48 benchmark functions with 7, 10, and 15 objectives are used to make comparisons with five representative many-objective optimization algorithms.**

***Index Terms*—Evolutionary algorithm, many-objective optimization, multistage optimization.**

AQ1 Manuscript received October 19, 2018; revised March 23, 2019; accepted July 17, 2019. This work was supported in part by the National Key Research and Development Program of China under Grant 2017YFC0804002, in part by the Program for Guangdong Introducing Innovative and Entrepreneurial Teams under Grant 2017ZT07X386, in part by the Shenzhen Peacock Plan under Grant KQTD2016112514355531, in part by the Science and Technology Innovation Committee Foundation of Shenzhen under Grant ZDSYS201703031748284, and in part by the Program for University Key Laboratory of Guangdong Province under Grant 2017KSYS008. This paper was recommended by Associate Editor B. Derbel. *(Corresponding author: Ran Cheng.)*

H. Chen is with the College of Systems Engineering, National University of Defense Technology, Changsha 410073, China (e-mail: hkchen@nudt.edu.cn).

R. Cheng is with the Shenzhen Key Laboratory of Computational Intelligence, University Key Laboratory of Evolving Intelligent Systems of Guangdong Province, Department of Computer Science and Engineering, Southern University of Science and Technology, Shenzhen 518055, China (e-mail: ranchengcn@gmail.com).

W. Pedrycz is with the Department of Electrical and Computer Engineering, University of Alberta, Edmonton, AB T6G 2V4, Canada, also with the Department of Electrical and Computer Engineering, Faculty of Engineering, King Abdulaziz University, Jeddah 21589, Saudi Arabia, and also with the Systems Research Institute, Polish Academy of Sciences, 01447 Warsaw, Poland (e-mail: wpedrycz@ualberta.ca).

Y. Jin is with the Department of Computer Science, University of Surrey, Guildford GU2 7XH, U.K. (e-mail: yaochu.jin@surrey.ac.uk).

Color versions of one or more of the figures in this paper are available online at http://ieeexplore.ieee.org.

Digital Object Identifier 10.1109/TSMC.2019.2930737

I. Introduction

Real-world optimization problems, such as parallel machine scheduling [1], hybrid electric vehicle optimization [2], and workflow scheduling in clouds [3], often need to simultaneously optimize multiple conflicting objectives, known as the multiobjective optimization problems (MOPs) [4], [5]

$$\begin{aligned} \text{Minimize} \quad & F(\mathbf{x}) = [f_1(\mathbf{x}), f_2(\mathbf{x}), \ldots, f_m(\mathbf{x})] \\ \text{s.t.} \quad & \mathbf{x} \in \Omega \end{aligned} \tag{1}$$

where $\mathbf{x} = (x_1, x_2, \ldots, x_n)$ represents the decision vector, and $\Omega \subseteq \mathbb{R}^n$ stands for the set of all the feasible decision vectors. The symbols n and m denote the number of decision variables and optimization objectives, respectively. The function $f_i(\mathbf{x})$ $\forall i \in \{1, 2, \ldots, m\}$ is used to map Ω to $\mathbb{R}$, i.e., $f_i : \Omega \rightarrow \mathbb{R}$. Specifically, an MOP with four or more objectives (i.e., $m \geq 4$) often refers to a many-objective optimization problem (MaOP) [6].

Due to the conflicts among the objectives of MOPs, improving one objective typically leads to the deterioration of the others [7]–[9]. Thus, there exists no single solution that can minimize all the objectives [10], [11], but a set of compromise solutions making tradeoffs among different objectives can be obtained. Regarding two solutions $\mathbf{x}_1, \mathbf{x}_2 \in \Omega$ of an MOP, $\mathbf{x}_1$ is considered to *dominate* $\mathbf{x}_2$ (expressed as $\mathbf{x}_1 \prec \mathbf{x}_2$) if $\mathbf{x}_1$ is better than or equal to $\mathbf{x}_2$ in all the objectives and $\mathbf{x}_1$ is strictly superior to $\mathbf{x}_2$ in at least one objective. One solution $\mathbf{x}^* \in \Omega$ is Pareto optimal if and only if there is no solution dominating it. In general, all the Pareto-optimal solutions comprise the Pareto optimal set, where the Pareto set (PS) and the Pareto-front (PF) are the images in the decision space and the objective space, respectively.

To obtain the Pareto optimal solutions for MOPs, a variety of multiobjective evolutionary algorithms (MOEAs) have been proposed over the past three decades [12], [13]. These existing algorithms are broadly divided into three categories: 1) Pareto dominance-based; 2) indicator-based; and 3) decomposition-based [12]. Pareto dominance-based MOEAs are often first sort the candidate solutions into many nondominated fronts, and then employ a secondary criterion to sort the solutions in the last accepted front. The classical works of this category are NSGA-II [14], MOPSO [15], etc. Regarding indicator-based MOEAs (e.g., HypE [16], AR-MOEA [17], BiGE [18], and others), a smaller number of indicators (e.g., one or two) related to the objective number are often used to sort the candidate solutions. For decomposition-based algorithms (e.g., MOEA/D and its variants [13], [19]–[21]), they partition the original MOP into many subproblems to be solved in a collaborative manner.

Although the existing MOEAs exhibit excellent performance in solving MOPs, their performance suffers from the curse of dimensionality with respect to the number of objectives in MaOPs, which can be attributed to three main reasons. First, the objective space of an MaOP expands exponentially with increasing number of objectives [22], [23], thus, resulting in a sparse distribution of the candidate solutions in the objective space, which poses a challenge to the diversity assessment [10]. Second, the increasing number of objectives leads to the dominance resistance [17], [24], [25], i.e., the percentage of nondominated candidate solutions in a population will sharply increase as the number of objectives, causing the failure of the dominance-based environmental selection strategies in MOEAs (e.g., NSGA-II, MOPSO, etc.) in distinguishing the candidate solutions. In addition, the PFs of MaOPs have various shapes, which will further challenge the tradeoffs between the convergence and the diversity. For example, some recent works have been demonstrated that the performance of the decomposition-based algorithms is greatly influenced by the PF shapes of MaOPs [17], [26].

To remedy the deficiency of MOEAs in solving the MaOPs, so far, a number of many-objective optimization algorithms (MaOEAs) have been reported [10], [12], [22], [27]. These MaOEAs typically follow the framework of MOEAs, mostly aiming to simultaneously strike a balance between convergence and diversity during the whole evolutionary process. However, as pointed in [10], despite that the convergence and diversity are two key factors to the performance of an MaOEA, they play different roles during different stages of the evolutionary process. Specifically, since the population of an MaOEA at the early search stage is still far from convergence, a higher convergence pressure is more desirable to push the population toward the PF. By contrast, at the later search stage, since the solutions are already near the PF, a wider spreading of the candidate solutions (i.e., diversity) is more preferable. Therefore, this motivates us to partition the whole evolutionary process into two stages, and the convergence is emphasized at the first stage, then the balance of convergence and diversity close to PF is emphasized at the second stage. This can avoid the negative effect of potential conflicts between the convergence and diversity. In summary, the key contributions of this paper are as follows.

1) A novel two-stage evolutionary algorithm, named TSEA, is proposed to partition the whole evolutionary search process into two stages. The first stage leverages multiple populations to accelerate the convergence toward the PF, followed by the balance of convergence and diversity at the second stage.
2) We design a novel environmental selection scheme for the second stage in TSEA to balance the convergence and diversity. This selection scheme evenly divides each objective dimension into a number of intervals and retains one candidate solution having the best convergence from each interval.
3) We conduct extensive experiments to compare the proposed TSEA with five representative algorithms on 48 test instances with various PF shapes, where the objective number ranges from 7 to 15. The experimental results demonstrate the superiorities of the proposed TSEA.

This paper is organized as follows. The recent works on MOEAs and MaOEAs are summarized in Section II. Then, the proposed TSEA is described in Section III, followed by extensive studies to verify and quantify the superiority of the TSEA. At last, Section V concludes this paper and provides a challenging direction.

II. Related Work

Over the past three decades, intensive attention has been given to the area of multiobjective evolutionary optimization, and a number of MOEAs have been developed and improved. Most existing MOEAs have focused on environmental selection strategies for balancing convergence and diversity. On the basis of the environmental selection strategies, the existing MOEAs are roughly grouped into the following three classes [12], [28]: 1) Pareto dominance-based; 2) indicator-based; and 3) decomposition-based.

For the Pareto dominance-based MOEAs, they first sort solutions into a series of nondominated levels are based on their dominance relationships, and then employ a secondary criterion to sort solutions in the last accepted level. The representative MOEAs of this category are the NSGA-II [14], PESA-II [29], MOPSO [15], and SPEA2 [30]. Besides, the Pareto dominance-based MOEAs have been widely used to solve various practical problems. For instance, Chen and Chou [31] modeled the crew roster recovery problems as multiobjective constrained combinational optimization problems and proposed a new version of the NSGA-II to search the Pareto solutions. To optimize the crude oil operations, Hou *et al.* [32] improved the NSGA-II using a new chromosome to model the feasible space. These algorithms show promising performance in solving problems having two or three objectives. Nevertheless, when increasing the number of objectives in MaOPs, the candidate solutions in a population often become incomparable with respect to their dominance relationships, which severely deteriorates their performances [25], [33]. To address the drawback of the Pareto dominance in distinguishing candidate solutions with many objectives, some new versions of Pareto dominance relation are designed, such as corner-sort-dominance [34], θ-dominance [33], grid-based dominance [35], fuzzy Pareto dominance [36], and alike. In addition, Chen *et al.* [37] proposed a hyperplane-assisted strategy to distinguish the nondominated solutions for many-objective optimization.

The indicator-based MOEAs often compare solutions using low-dimensional indicators (e.g., a single indicator [17] or two indicators [18]) instead of using their objective vectors directly. For instance, Zitzler and Künzli [38] defined a binary performance indicator to measure the solutions, and then designed a framework for indicator-based evolutionary algorithms. Beume *et al.* [39] combined the hypervolume indicator and the concept of nondominated sorting to form a selection strategy. However, the computation of the hypervolume indicator is time consuming when the number of objectives is large. To reduce the computational time of hypervolume, Bader and Zitzler [16] employed the Monte Carlo simulation for the hypervolume calculation. Bringmann *et al.* [40] empirically analyzed the performance impact of hypervolume-based Monte Carlo approximations on MOEAs, and concluded that the performance of MOEAs does not suffer from the inexact hypervolume. However, with the increasing number of objectives, the hypervolume calculation is still considerably expensive. Recently, Tian *et al.* [17] developed a new MOEA on the basis of an improved inverted generational distance indicator, and then designed a strategy to adaptively alter the reference vectors according to the indicator contributions of candidate solutions in the external archive. Zhou *et al.* [41] designed a co-guided MaOEA and used an indicator $_{\varepsilon+}I$ and reference points to improve the convergence and diversity. Li *et al.* [18] designed two indicators to, respectively, measure the convergence and diversity of the candidate solutions, and then employed the nondominated sorting method to balance the convergence and diversity based on these two indicators.

The decomposition-based MOEAs employ a set of weight vectors to decompose the MOP into a number of subproblems, which are solved in a collaborative way [13]. For instance, Zhang and Li [19] suggested the MOEA/D, which is among the most representative algorithms of this type. Wang *et al.* [42] suggested a preference-inspired algorithm to search interesting solutions for decision makers. Li *et al.* [43] combined the dominance-based strategy into the decomposition-based MOEAs to achieve good tradeoffs between the convergence and diversity. To adapt the MOEA/D to deal with the MOPs having complex PF shapes, Qi *et al.* [44] designed a strategy to adaptively adjust the weight vectors according to the geometric relationship between the weight vectors and the optimal solutions. Wang *et al.* [9] also proposed an adaptive adjustment strategy to adjust weight vectors for MOEA/D on the basis of the distribution of population located in the objective space. Wang *et al.* [45] demonstrated the importance of p-value in the L_p methods and designed a Pareto adaptive scalarizing strategy to find the near-optimal p-value. Cai *et al.* [46] suggested to use the angles between the objective vectors to improve the performance of MOEA/D in maintaining diversity. Cai *et al.* [47] proposed a constrained decomposition with grids to avoid the decomposition-based MOEAs being sensitive to the shapes of PFs. Elarbi *et al.* [48] designed a decomposition-based dominance relation and a diversity measurement for many-objective optimization. Wang *et al.* [49] used a localized weighted sum strategy to improve the performance decomposition-based MOEA in solving nonconvex problems.

A new direction of the decomposition-based approach is to divide the objective space of an MOP into many subspaces using a set of reference vectors, and then evolve the subpopulation belonging to each subspace cooperatively. The classical algorithms in this branch are the MOEA/D-M2M [20], MOEA/D-AM2M [50], and RVEA [10]. Chen *et al.* [51] proposed an indicator to measure the contribution of each subspace, and then designed an adaptive strategy to allocate computational resources for each subspace. To deal with the complicated PF shapes, Liu *et al.* [50] designed a new strategy to dynamically adjust the subregions of each subproblem on the basis of the obtained solutions. Kang *et al.* [52] improved the MOEA/D-M2M by designing a strategy to dynamically distribute computational resources to each subproblem according to their frequency of updating the external archive.

In summary, the aforementioned MOEAs strive to improve the population convergence and diversity simultaneously during the whole evolutionary process. However, emphasizing diversity during the early search stage will naturally weaken population convergence toward the PF, which is particularly serious when the PF has a complex shape. To address this issue, there also exist several works dedicated to solve MaOPs by multistage strategies. For instance, Cai *et al.* [53] improved the MOEA/D using a new strategy that first optimizes the boundary subproblems to obtain the corner solutions, then conducts the explorative search to extend the PF approximation. Hu *et al.* [54] designed a two-stage strategy to first obtain several extreme Pareto-optimal solutions, and then extend these obtained solutions to approximate the PF. In addition, Sun *et al.* [55] developed a two-stage strategy that strengthens the convergence at the first stage using an aggregation method, and then improves diversity using the decomposition-based approach. Similar to the above works, the proposed TSEA in this paper also partitions the whole evolutionary process into two stages. Different from these existing works, the first stage is proposed to push multiple subpopulations to different areas of the PF, and then at the second stage, a new environmental selection strategy is designed to balance convergence and diversity close to the PF.

So far, the angle-based methods have been widely used to measure the diversity of the candidate solutions. For example, the acute angles between solutions and reference vectors were used to associate solutions to different subspaces to maintain the population diversity [10], [20], [50]. Besides, the angles among solutions in objective space were utilized to measure the diversity of solutions [25], [56]. In the proposed TSEA, the angles between the solutions are also used as the diversity measurement. In addition, a new selection strategy is designed for TSEA to select solutions from each objective dimension, such that it can strike a good balance between convergence and diversity.

III. TWO-STAGE EVOLUTIONARY ALGORITHM

The proposed algorithm TSEA is detailed in this section. First, the main procedure of algorithm TSEA is given. Then, we describe the proposed two-stage evolutionary strategy. In the sequential, the novel environmental selection strategy is elaborated.

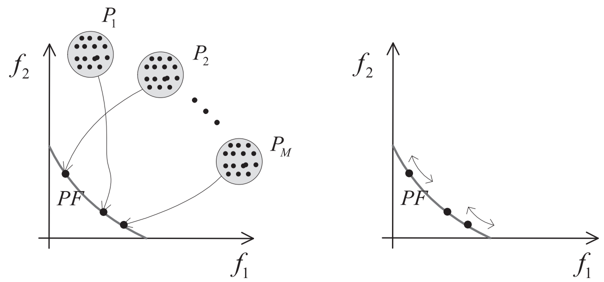

(a) (b)

Fig. 1. Illustration of the proposed two-stage strategy. (a) At stage one, the subpopulations $P_1, P_2, \ldots, P_M$ are pushed close to the PF with respect to a set of weight vectors and (b) at stage two, the candidate solutions are diversified near the PF.

A. Main Procedure of TSEA

Before describing the proposed TSEA in detail, we provide a visual example in Fig. 1 to illustrate the main idea. The stage one of TSEA will randomly initialize a series of subpopulations, denoted by $P_1, P_2, \ldots, P_M$ in Fig. 1(a), and then pushes these subpopulations to different area of PF with respect to a set of weight vectors. After that the TSEA enters stage two to diversify the candidate solutions near the PF, which is shown in Fig. 1(b).

The framework of the algorithm TSEA is given in Algorithm 1. The main inputs of TSEA are: the optimization problem; the maximum number of function evaluations; the size of the output population; the number of subpopulations and the size of each subpopulation; and the convergence threshold Δ for subpopulations. Similar to other evolutionary algorithms [10], [22], the output of algorithm TSEA is the final population with N individuals.

As shown in Algorithm 1, the proposed TSEA first finds the diversity-related decision variables, and the set $\mathbf{I}_d$ is used to record all the diversity-related variables (line 1). Similar to [57] and [58], a decision variable is defined as diversity related if perturbing it only generates nondominated solutions. Then, M subpopulations with a size of N' are generated randomly (lines 3 and 4). To accelerate the convergence of each subpopulation toward the PF at the first stage, each subpopulation merely emphasizes the convergence, and we use different weight vectors to guide them toward different areas of the PF. Thus, an m-dimensional weight vector between 0 and 1 is randomly generated for each subpopulation (line 5). The arrays *bestF* and *conT* are used to record the best fitness and convergence status of each subpopulation (line 7). For each subpopulation, the well-known simulated binary crossover (SBX) and the polynomial mutation (PM) operators are applied to generate a new subpopulation (line 12). With respect to the subpopulation P_k, if the new solution in the new subpopulation Q_k has better fitness, it will replace the original solution in P_k (lines 13–15). The fitness of a solution p coming from subpopulation P_k is defined as $\mathrm{Fit}(p) = \sum_{i=1}^{m} W_{k,i} \cdot f_i$, where $W_{k,i}$ represents the ith element of weight vector W_k, and f_i denotes the ith objective value of solution p. Note that p_k^j and q_k^j represent the jth solution in P_k and Q_k, respectively (line 14). In addition, the best fitness of a subpopulation P_k is denoted as bestFit(P_k), i.e., $\mathrm{bestFit}(P_k) = \min_{p \in P_k} \mathrm{Fit}(p)$. For a subpopulation, it is deemed to be converged in case the improvement of the best fitness among all the individuals is lower than the predetermined threshold Δ (line 16).

After all the subpopulations at the first stage have converged, all the nondominated solutions coming from the M subpopulations are selected to form a new population R (lines 18 and 19). Then, the algorithm enters the second stage (lines 22–24). During each iteration at this stage, a new population R is generated by applying SBX and PM operators on diversity-related variables $\mathbf{I}_d$ (line 23). Afterward, an environmental selection strategy is triggered to improve the population diversity (line 24), which is detailed in Algorithm 2.

Algorithm 1: Main Procedure of the Proposed TSEA

Input: MaOP; maximal number of function evaluations (*MFEs*); population size N; number of subpopulations M; subpopulation size N'; threshold Δ;
Output: The final population A;
1 $\mathbf{I}_d \leftarrow$ Find the diversity-related variables;
2 Initialize the used function evaluations as $FEs \leftarrow 0$;
3 **for** $k = 1 \rightarrow M$ **do**
4 Initialize a subpopulation P_k with size N' randomly;
5 Randomly generate a m-dimensional vector W_k between 0 and 1;
6 $A \leftarrow \emptyset$;
7 $bestF_{1\times M} \leftarrow +\infty$; $conT_{1\times M} \leftarrow$ **FALSE**;
8 **while** $FEs < MFEs$ **do**
9 **for** $k = 1 \rightarrow M$ **do**
10 **if** $conT(k) ==$ ***TRUE*** **then**
11 **CONTINUE**;
12 $Q_k \leftarrow$ SBX+PM(P_k);
13 **for** $j = 1 \rightarrow N'$ **do**
14 **if** $Fit(p_k^j) \geq Fit(q_k^j)$ **then**
15 $p_k^j \leftarrow q_k^j$;
16 **if** $|bestFit(P_k) - bestF(k)| < \Delta$ **then**
17 $conT(k) \leftarrow$ **TRUE**;
18 $A \leftarrow A \bigcup P_k$;
19 Update A by removing dominated solutions;
20 **else**
21 $bestF(k) \leftarrow bestFit(P_k)$;
22 **if** *all the elements in conT are* ***TRUE*** **then**
23 $R \leftarrow$ Apply SBX and PM operator on $\mathbf{I}_d$ of A;
24 $A \leftarrow EnvironmentalSelection(A \bigcup R, N)$;

B. Environmental Selection Approach

As shown in Algorithm 2, the proposed environmental selection strategy employs a three-step policy: 1) the first step is to remove dominated solutions from the combined population (line 1); 2) the second step evenly selects candidate solutions from each objective dimension (lines 2–16); and 3) the third step retains candidate solutions according to the cosine values

Algorithm 2: *EnvironmentalSelection*(Q, N)

Input: Combined population Q; size of population N;
Output: A selected population A;
1 Discard all the dominated solutions from Q;
2 $A \leftarrow \varnothing$; $S \leftarrow \varnothing$;
3 $T \leftarrow \lfloor \frac{N}{m} \rfloor$;
4 **for** $j = 1 \rightarrow m$ **do**
5   $l \leftarrow$ The minimal value in the j-th objective of population Q;
6   $u \leftarrow$ The maximal value in the j-th objective of population Q;
7   $len \leftarrow \frac{u-l}{T-1}$;
8   **for** $t = 1 \rightarrow T$ **do**
9     $I \leftarrow \varnothing$;
10   **for** $i = 1 \rightarrow |Q|$ **do**
11   **if** $l + (t-1) \times len \leqslant F_{i,j} < l + t \times len$ **then**
12         $I \leftarrow I \bigcup \{i\}$;
13   **if** $I != \varnothing$ & $I \bigcap S == \varnothing$ **then**
14       $i \leftarrow$ Select the solution having the minimal sum of objective values among the set I;
15       $S \leftarrow S \bigcup \{i\}$;
16       $A \leftarrow A \bigcup Q(i)$;
17 $Q \leftarrow Q \setminus A$;
18 **while** $|P| < N$ & $Q! = \varnothing$ **do**
19   $minCos \leftarrow 1$; $s \leftarrow 1$;
20   **for** $i = 1 \rightarrow |Q|$ **do**
21     $maxCos \leftarrow 0$;
22   **for** $j = 1 \rightarrow |P|$ **do**
23       $cos\theta_{i,j} \leftarrow$ Calculate the cosine between solution $Q(i)$ and $P(i)$;
24   **if** $maxCos < cos\theta_{i,j}$ **then**
25         $maxCos \leftarrow cos\theta_{i,j}$;
26   **if** $maxCos < minCos$ **then**
27       $minCos \leftarrow maxCos$; $s \leftarrow i$;
28   $A \leftarrow A \bigcup Q(s)$;
29   $Q \leftarrow Q \setminus Q(s)$;
30 Return the selected population A;

of the angles between the selected candidate solutions and the remaining ones (lines 17–29).

The set A, which is used to record the selected candidate solutions, is initialized as empty (line 2). Then, the set S is also initialized as empty (line 2), and it is used to record the indices of the selected solutions in the second step. Next, the number of solutions that are selected from each objective dimension is computed and denoted as T (line 3). Then, the objective values in each dimension are evenly divided into T intervals. For each interval, if there is no candidate solution selected in it (line 13), the one having the best convergence will be selected then (line 14), where the convergence is defined as the sum of its objective values. In addition, the symbol $F_{i,j}$ represents the value of the jth objective of the ith candidate solution in the population Q.

Afterward, all the selected candidate solutions are removed from Q (line 17), and the environmental selection strategy enters the third step, which will be iterated until the number of the selected candidate solutions $|P|$ reaching the population size N or the set Q becomes empty (line 18). During each iteration, the environmental selection strategy associates each remaining candidate solution with the maximal cosine value between it and all the selected candidate solutions (lines 21–25), and then selects the candidate solution having the minimal associated cosine value (lines 26 and 27). Next, the selected candidate solution will be added to the set A (line 28) and discarded from the set Q (line 29). Once the number of the selected candidate solutions reaches the population size or the set Q becomes empty, the third step will stop iterating and the selected population A will be returned (line 30).

IV. Experimental Studies

To quantitatively verify the effectiveness of the proposed TSEA, it is compared with five representative algorithms for many-objective optimization: 1) NSGA-III [22]; 2) RVEA [10]; 3) MaOEA-R&D [59]; 4) VaEA [25]; and 5) SPEA/R [27]. The five algorithms are briefly described as follows.

NSGA-III is the tailored version of the NSGA-II [14]. In *NSGA-III*, a new reference vector-based scheme is developed to strengthen the convergence when selecting candidate solutions in the last accepted front.

RVEA employs a set of reference vectors to divide the objective space of an MOP into a number of subspaces and associates each candidate solution with a reference vector having the minimal angle. Also, a new indicator, namely, angle penalized distance, is proposed to sort all the solutions in a subspace. Besides, the *RVEA* includes a strategy to adaptively adjust reference vectors according to the distribution of the candidate solutions.

MaOEA-R&D first searches for several solutions along m directions and construct the objective space boundary, and then adopts a diversity improvement strategy to improve the population diversity within the objective space boundary.

VaEA first employs the nondominated sorting approach to divide the candidate solutions into a number of fronts. For the solutions in the last accepted front, the solution having the largest acute angle to the selected solutions is iteratively selected until the number of selected solutions reaches the population size.

SPEA/R proposes a reference-based density assessment method and a fitness calculation method, then employs the diversity-first-and-convergence-second strategy to balance the convergence and diversity.

For these five algorithms in comparison, their source codes have been embedded into the PlatEMO,[1] which is an open-source MATLAB-based platform for multiobjective evolutionary optimization. The experiments in this paper follow the

[1] https://github.com/BIMK/PlatEMO

settings of these algorithms and problems in their published edition.

A. Experimental Settings

1) Benchmark Problems: To compare the performance of the six MOEAs, we utilize the following 16 benchmark functions: MaF1–MaF7 [60] and WFG1–WFG9 [57]. The benchmark functions MaF1–MaF7, which are specially designed for evaluating many-objective optimization, cover diverse properties, e.g., complicated Pareto front shapes, search landscapes, and alike. In addition, the nine benchmarks WFG1–WFG9 in the second test suite are widely used in the existing literature. In the experiments, a test instance refers to an MaOP with a specific number of objectives, e.g., benchmark WFG1 with seven objectives.

2) Performance Indicators: The hypervolume (HV) [61] and inverted generational distance (IGD) [62] are two widely used indicators to measure the effectiveness of MOEAs. The experimental studies in this paper also utilize them to compare the effectiveness of the six algorithms.

1) *HV:* It is defined as the volume of space, which consists of a reference point and all the output solutions in the objective space. The larger HV value means the better performance of the corresponding algorithm with respect to both the convergence and diversity. For each test instance, we set the reference point as 1.5 times of the upper bounds of its PF.
2) *IGD:* For an output population P, this metric is generally defined as

$$\mathrm{IGD}(P) = \frac{\sum_{v \in P^*} d(v, P)}{|P^*|} \tag{2}$$

where P^* stands for a set of sample Pareto optimal solutions on the PF, and $d(v, P)$ is the minimal distance between point v and all the points in P. Based on the definition in (2), a lower IGD value indicates the better performance of the corresponding algorithm. In our experiments, the P^* is set to contain around 8000 points for each test instance.

3) General Settings: For fair comparisons, the population sizes and termination conditions are set as follows.

1) *Population Size:* Similar to the existing works [10], [22], [25], [27], [59], the population size of the six algorithms is set according to the number of objectives of the test instances, i.e., 168, 230, and 240 for problems with 7, 10, and 15 objectives, respectively.
2) *Termination Condition:* For all the six algorithms, their termination conditions are set as the maximum number of function evaluations, i.e., 800 000 for MaF3 and MaF4; and 400 000 for the other benchmark functions.

B. Experimental Results

For statistical comparisons, the mean and standard deviation (in parentheses) of the HV and IGD values on all the test instances are summarized in Tables I and II, respectively. The Wilcoxon rank-sum test with $\alpha = 0.05$ is employed to verify the significant differences. The symbols $-$, $+$, and $\approx$ indicate that the indicator value of the corresponding algorithm has significantly worse, better, and similar performance in comparison with the proposed TSEA, respectively. For each test instance, the best HV and IGD values are highlighted.

The HV values of the six algorithms on the 16 benchmark functions with 7, 10, and 15 objectives are reported in Table I. From these experimental results, in summary, we can observe that the proposed TSEA shows generally the better performance in comparison with the other five algorithms with respect to the HV indicator. For the 48 test instances, TSEA significantly performs the best on 33 of them. To be specific, the TSEA outperforms *NSGA-III*, *RVEA*, *MaOEA-R&D*, *VaEA*, and *SPEA/R* on 43, 42, 48, and 36 of 34 test instances, respectively. Such better results illustrate the superiorities of the proposed TSEA with respect to both the convergence and diversity.

For the MaF test instances, except three test instances, namely, 7-objective MaF5, 10-objective MaF5, and 15-objective MaF7, the proposed TSEA generates significantly higher HV than the other algorithms on all the other test instances. For example, the HV value obtained by TSEA on 7-objective MaF1 on average is higher than algorithms *NSGA-III*, *RVEA*, *MaOEA-R&D*, *VaEA*, and *SPEA/R* by 74.06%, 358.42%, 1096.38%, 3.81%, and 371.97%, respectively. This is due to the fact that the stage one of TSEA only focuses on the population convergence and thus accelerates the convergence speed by avoiding the negative influence of the complicated PF shapes. By contrast, for the five algorithms in comparison, they employ the framework of traditional MOEAs to form tradeoffs between the population convergence and diversity simultaneously during the whole search process, which fails to work properly on problems with complicated PF shapes.

The WFG1–WFG9 benchmark functions are widely used to assess the effectiveness of MOEAs in solving many-objective problems. To further test the effectiveness of the algorithm TSEA, these 9 test functions with 7, 10, and 15 objectives are also used in the experimental comparisons. As shown in Table I, algorithm TSEA still significantly performs better than the five comparative algorithms on more than half of the test instances. Compared with *SPEA/R*, the proposed TSEA generates significantly higher HV values on 16 out of the 27 test instances. Regarding the *NSGA-III*, *RVEA*, *MaOEA-R&D*, and *VaEA*, the proposed TSEA performs better on even more instances.

For IGD indicator, the results of the six algorithms are summarized in Table II. Among the 48 test instances, the proposed TSEA generates significantly lower IGD values than *NSGA-III*, *RVEA*, *MaOEA-R&D*, *VaEA* and *SPEA/R* on 41, 39, 41, 27, and 35 test instances, respectively. In summary, TSEA outperforms the five compared algorithms on 25 out of the 48 test instances with respect to IGD indicator. These results again illustrate the promising performance of the algorithm TSEA.

To visually illustrate the distribution of the solution sets obtained by the six algorithms, we choose four test instances, AQ2 i.e., MaF1, MaF6, and WFG3 with ten objectives, to depict the objective vectors in parallel coordinates. For each algorithm, the solution sets with the lowest IGD value among 30 runs are shown in Figs. 2–4.

TABLE I
HV VALUES OF THE SIX ALGORITHMS ON BENCHMARK FUNCTIONS MAF1–MAF7 AND WFG1–WFG8 WITH 7, 10, AND 15 OBJECTIVES

MaOP	m	*NSGA-III*	*RVEA*	*MaOEA-R&D*	*VaEA*	*SPEA/R*	*TSEA*
MaF1	7	2.66e-1 (1.64e-2)−	1.01e-1 (2.76e-2)−	3.87e-2 (2.13e-3)−	4.46e-1 (4.29e-3)−	9.81e-2 (1.51e-2)−	4.63e-1 (3.98e-3)
	10	4.16e-2 (2.92e-3)−	1.06e-2 (1.87e-3)−	4.95e-3 (2.37e-4)−	1.02e-1 (2.39e-3)−	1.39e-2 (3.83e-3)−	1.07e-1 (2.46e-3)
	15	1.26e-3 (1.08e-4)−	2.85e-4 (6.01e-5)−	1.61e-4 (1.59e-5)−	5.06e-3 (1.72e-3)−	2.63e-4 (3.91e-5)−	5.62e-3 (1.09e-3)
MaF2	7	8.12e-1 (2.28e-2)−	6.94e-1 (5.36e-2)−	3.76e-1 (2.30e-2)−	8.95e-1 (7.29e-3)−	7.27e-1 (8.64e-2)−	9.23e-1 (3.62e-3)
	10	3.41e-1 (1.09e-2)−	2.68e-1 (4.79e-2)−	1.51e-1 (2.13e-2)−	3.46e-1 (2.60e-3)−	3.27e-1 (2.53e-3)−	3.60e-1 (1.76e-3)
	15	1.19e-2 (7.53e-4)−	7.57e-3 (3.79e-4)−	7.25e-3 (1.26e-3)−	1.15e-2 (1.08e-4)−	8.32e-3 (8.49e-4)−	1.55e-2 (1.07e-4)
MaF3	7	1.70e+1 (6.44e-3)−	1.70e+1 (2.41e-2)−	1.69e+1 (1.02e-1)−	1.56e+1 (1.49e+0)−	1.55e+1 (1.26e+0)−	1.71e+1 (1.91e-5)
	10	4.40e+1 (2.17e+1)−	5.76e+1 (4.29e-2)−	5.72e+1 (3.67e-1)−	5.70e+1 (1.05e+0)−	0.00e+0 (0.00e+0)−	5.77e+1 (3.6e-14)
	15	2.30e+2 (2.10e+2)−	4.37e+2 (1.07e-1)−	4.33e+2 (2.57e+0)−	1.50e+2 (1.90e+2)−	0.00e+0 (0.00e+0)−	4.38e+2 (1.2e-13)
MaF4	7	3.48e+8 (2.70e+7)−	6.30e+7 (1.10e+7)−	6.58e+7 (1.72e+7)−	4.54e+8 (1.87e+7)−	1.64e+8 (8.19e+7)−	4.76e+8 (6.76e+6)
	10	1.80e+16 (8e+14)−	1.15e+15 (4e+14)−	3.47e+15 (1e+15)−	2.45e+16 (1e+15)−	1.01e+16 (3e+15)−	2.59e+16 (6e+14)
	15	8.56e+34 (6e+33)−	9.35e+32 (1e+32)−	4.76e+34 (4e+34)−	1.02e+35 (1e+34)−	1.64e+34 (1e+34)−	1.13e+35 (7e+33)
MaF5	7	4.52e+9 (5.90e+5)≈	4.49e+9 (4.61e+7)−	4.33e+9 (4.51e+7)−	4.52e+9 (2.91e+6)≈	4.53e+9 (7.45e+5)+	4.52e+9 (1.31e+6)
	10	2.07e+18 (8e+13)≈	2.07e+18 (1e+15)≈	1.98e+18 (2e+16)−	2.07e+18 (4e+14)≈	2.07e+18 (1e+14)≈	2.07e+18 (1e+14)
	15	5.81e+38 (1e+35)−	5.81e+38 (2e+35)−	5.63e+38 (7e+36)−	5.81e+38 (1e+34)−	5.80e+38 (2e+34)−	5.82e+38 (4e+36)
MaF6	7	5.98e-3 (9.91e-5)−	5.76e-3 (6.34e-5)−	5.56e-3 (1.92e-7)−	6.03e-3 (1.15e-4)−	5.75e-3 (3.85e-5)−	6.05e-3 (7.61e-6)
	10	8.83e-7 (1.38e-6)−	3.76e-6 (1.37e-6)−	4.57e-6 (6.89e-9)−	4.40e-6 (1.57e-7)−	4.39e-6 (8.38e-7)−	4.78e-6 (6.89e-9)
	15	2.10e-15 (5e-15)−	3.25e-14 (9e-17)−	3.23e-14 (8e-17)−	3.08e-14 (1e-15)−	2.08e-15 (7e-15)−	3.30e-14 (5e-17)
MaF7	7	4.62e+1 (6.36e-1)−	4.38e+1 (5.93e-1)−	3.48e+1 (1.13e+0)−	4.67e+1 (2.40e-1)−	4.58e+1 (6.47e-1)−	4.73e+1 (2.78e-1)
	10	1.35e+2 (1.99e+0)−	1.13e+2 (2.28e+0)−	7.28e+1 (6.65e+0)−	1.35e+2 (1.12e+0)−	1.35e+2 (1.44e+0)−	1.38e+2 (7.48e-1)
	15	3.25e+2 (4.34e+1)−	1.94e+2 (9.85e+1)−	5.18e+1 (4.60e+1)−	6.56e+2 (4.77e+0)+	3.89e+2 (3.23e+2)−	6.49e+2 (2.20e+1)
WFG1	7	8.47e+6 (3.54e+5)−	8.93e+6 (5.11e+5)−	6.20e+6 (1.61e+6)−	1.05e+7 (2.67e+2)+	1.05e+7 (3.04e+1)+	9.71e+6 (6.07e+5)
	10	1.50e+11 (8.8e+9)−	1.84e+11 (9.5e+9)+	9.76e+10 (1e+10)−	1.92e+11 (8.9e+6)+	1.92e+11 (3.4e+5)+	1.74e+11 (1e+10)
	15	1.21e+19 (9e+17)−	1.40e+19 (6e+17)+	7.44e+18 (1e+18)−	1.46e+19 (3e+14)+	1.46e+19 (5e+13)+	1.32e+19 (1e+18)
WFG2	7	1.09e+7 (1.50e+4)−	1.08e+7 (4.13e+4)−	1.06e+7 (1.52e+5)−	1.09e+7 (6.06e+3)−	1.02e+7 (1.43e+3)−	1.10e+7 (5.23e+3)
	10	2.13e+11 (3.3e+8)−	2.11e+11 (7.3e+8)−	2.08e+11 (3.1e+9)−	2.13e+11 (1.4e+8)−	2.14e+11 (6.0e+7)−	2.15e+11 (1.2e+8)
	15	1.86e+19 (3e+16)−	1.83e+19 (1e+17)−	1.83e+19 (1e+17)−	1.87e+19 (1e+16)≈	1.87e+19 (1e+16)≈	1.87e+19 (7e+15)
WFG3	7	1.64e+0 (7.57e-1)−	2.50e-1 (4.98e-1)−	0.00e+0 (0.00e+0)−	3.45e+0 (3.02e-1)−	3.11e+0 (3.53e-1)−	4.68e+0 (1.44e-1)
	10	3.49e-5 (1.12e-4)−	0.00e+0 (0.00e+0)−	0.00e+0 (0.00e+0)−	3.11e-3 (4.35e-4)−	2.22e-3 (1.10e-3)−	4.09e-3 (6.09e-4)
	15	0.00e+0 (0.00e+0)−	0.00e+0 (0.00e+0)−	0.00e+0 (0.00e+0)−	0.00e+0 (0.00e+0)−	8.05e-16 (4e-15)−	9.27e-14 (6e-14)
WFG4	7	1.07e+7 (3.40e+4)−	1.06e+7 (4.01e+4)−	8.74e+6 (4.55e+5)−	1.08e+7 (7.29e+3)−	1.08e+7 (1.95e+3)−	1.09e+7 (7.10e+3)
	10	2.10e+11 (1.0e+9)−	2.09e+11 (6.7e+8)−	1.71e+11 (1e+10)−	2.12e+11 (2.1e+8)−	2.13e+11 (2.2e+7)−	2.14e+11 (2.2e+7)
	15	1.80e+19 (2e+17)−	1.82e+19 (9e+16)−	1.61e+19 (6e+17)−	1.86e+19 (2e+16)−	1.87e+19 (1e+16)−	1.88e+19 (5e+14)
WFG5	7	1.03e+7 (6.45e+3)−	1.04e+7 (6.84e+3)≈	8.19e+6 (2.66e+5)−	1.04e+7 (6.60e+3)≈	1.04e+7 (1.52e+3)≈	1.04e+7 (1.65e+5)
	10	2.03e+11 (1.1e+8)−	2.03e+11 (1.0e+8)−	1.49e+11 (9.5e+9)−	2.03e+11 (9.9e+7)−	2.03e+11 (8.1e+6)−	2.04e+11 (2.5e+7)
	15	1.74e+19 (1e+17)−	1.76e+19 (3e+16)−	1.41e+19 (1e+18)−	1.77e+19 (8e+15)−	1.77e+19 (3e+15)−	1.78e+19 (2e+16)
WFG6	7	1.01e+7 (1.31e+5)−	1.01e+7 (1.91e+5)−	7.71e+6 (5.17e+5)−	1.03e+7 (1.37e+5)−	1.03e+7 (1.32e+5)−	1.05e+7 (1.65e+5)
	10	1.98e+11 (3.8e+9)−	1.98e+11 (4.6e+9)−	1.49e+11 (1e+10)−	2.00e+11 (2.0e+9)−	2.04e+11 (2.9e+9)≈	2.04e+11 (5.0e+9)
	15	1.68e+19 (3e+17)−	1.69e+19 (4e+17)−	1.40e+19 (1e+18)−	1.75e+19 (2e+17)≈	1.75e+19 (2e+17)≈	1.75e+19 (5e+17)
WFG7	7	1.07e+7 (2.65e+4)−	1.07e+7 (2.84e+4)−	7.61e+6 (4.97e+5)−	1.08e+7 (3.99e+3)−	1.08e+7 (1.66e+3)−	1.09e+7 (2.56e+3)
	10	2.12e+11 (5.5e+8)−	2.12e+11 (3.7e+8)−	1.23e+11 (8.2e+9)−	2.13e+11 (3.3e+7)−	2.13e+11 (9.5e+6)−	2.14e+11 (1.5e+7)
	15	1.84e+19 (1e+17)−	1.79e+19 (3e+17)−	1.03e+19 (1e+18)−	1.87e+19 (1e+15)−	1.87e+19 (6e+15)−	1.88e+19 (4e+14)
WFG8	7	1.02e+7 (4.31e+4)−	9.55e+6 (4.25e+5)−	7.31e+6 (9.38e+5)−	1.03e+7 (3.35e+4)−	1.05e+7 (8.80e+4)+	1.04e+7 (6.92e+4)
	10	2.02e+11 (3.3e+9)−	1.83e+11 (1e+10)−	1.50e+11 (2e+10)−	2.07e+11 (6.0e+8)−	2.12e+11 (9.3e+8)+	2.09e+11 (2.1e+8)
	15	1.61e+19 (1e+18)−	1.53e+19 (1e+18)−	1.38e+19 (1e+18)−	1.84e+19 (6e+16)−	1.82e+19 (2e+17)−	1.86e+19 (6e+16)
WFG9	7	1.01e+7 (3.07e+5)≈	1.03e+7 (9.77e+4)+	7.54e+6 (3.89e+5)−	1.03e+7 (3.99e+5)+	1.04e+7 (1.24e+5)+	1.01e+7 (5.96e+5)
	10	1.97e+11 (9.5e+9)+	1.97e+11 (5.7e+9)+	1.39e+11 (1e+10)−	1.99e+11 (1e+10)+	2.07e+11 (1.0e+9)+	1.92e+11 (1e+10)
	15	1.77e+19 (7e+17)+	1.63e+19 (7e+17)−	1.249e+19 (1e+18)−	1.76e+19 (6e+17)+	1.76e+19 (2e+17)+	1.65e+19 (1e+18)

As shown in Fig. 2, the distribution of the output solution sets of the six algorithms is quite different. Fig. 2(a) shows that *NSGA-III* has good convergence and diversity in the first, second, third, and fifth objectives. For *RVEA*, the size of the solution set is much smaller than the predefined population size, referring to Fig. 2(b). The reason is that *RVEA* decomposes the objective space into a series of subspaces, and each subspace will retain at most one candidate solution. However, on the problems with complicated PF shapes, some subspaces may contain more than one representative candidate solutions, while some subspaces are completely empty. Except the sixth and seventh objectives, the convergence and diversity

TABLE II
IGD VALUES OF THE SIX ALGORITHMS ON BENCHMARK FUNCTIONS MAF1–MAF7 AND WFG1–WFG8 WITH 7, 10, AND 15 OBJECTIVES

MaOP	m	*NSGA-III*	*RVEA*	*MaOEA-R&D*	*VaEA*	*SPEA/R*	*TSEA*
MaF1	7	2.38e-1 (1.23e-2)−	4.95e-1 (7.87e-2)−	5.48e-1 (4.78e-2)−	1.81e-1 (8.45e-4)−	4.32e-1 (6.97e-2)−	1.79e-1 (1.50e-3)
	10	2.82e-1 (1.45e-2)−	5.73e-1 (9.08e-2)−	5.65e-1 (4.01e-2)−	2.41e-1 (1.69e-3)−	4.83e-1 (4.79e-2)−	2.40e-1 (2.18e-3)
	15	3.13e-1 (8.02e-3)−	6.40e-1 (7.20e-2)−	5.85e-1 (3.55e-2)−	2.78e-1 (1.12e-3)+	6.12e-1 (5.02e-2)−	3.02e-1 (3.74e-3)
MaF2	7	1.60e-1 (8.11e-3)−	2.31e-1 (7.29e-2)−	7.89e-1 (4.21e-2)−	1.48e-1 (3.35e-3)−	2.08e-1 (1.26e-1)−	1.47e-1 (2.64e-3)
	10	2.09e-1 (2.42e-2)−	4.52e-1 (2.10e-1)−	8.15e-1 (5.41e-2)−	1.86e-1 (3.29e-3)−	1.96e-1 (4.23e-4)−	1.85e-1 (3.14e-3)
	15	2.14e-1 (9.25e-3)−	4.95e-1 (1.43e-1)−	8.33e-1 (7.92e-2)−	2.04e-1 (2.13e-3)−	6.57e-1 (1.02e-1)−	1.98e-1 (2.25e-3)
MaF3	7	1.10e-1 (1.72e-2)−	9.27e-2 (4.36e-3)−	1.99e-1 (3.59e-2)−	2.88e-1 (9.34e-2)−	5.82e-1 (1.59e-1)−	7.56e-2 (6.42e-4)
	10	2.45e+0 (6.75e+0)−	8.29e-2 (9.59e-3)−	1.98e-1 (3.25e-2)−	1.95e-1 (2.86e-2)−	6.51e+4 (1.10e+5)−	6.95e-2 (4.80e-4)
	15	6.36e+1 (1.83e+2)	9.21e-2 (4.23e-3)−	2.12e-1 (3.37e-2)−	2.85e+0 (5.49e+0)−	2.15e+5 (3.05e+5)−	7.20e-2 (8.61e-5)
MaF4	7	1.30e+1 (1.12e+0)−	2.59e+1 (8.13e+0)−	6.16e+1 (5.19e+0)−	8.57e+0 (4.74e-1)−	2.33e+1 (6.05e+0)−	8.10e+0 (3.16e-1)
	10	9.58e+1 (8.05e+0)−	2.06e+2 (6.45e+1)−	5.22e+2 (4.72e+1)−	5.67e+1 (1.26e+1)−	1.35e+2 (3.21e+1)−	5.12e+1 (1.66e+0)
	15	3.75e+3 (2.43e+2)−	7.96e+3 (1.57e+3)−	1.49e+4 (4.11e+3)−	1.37e+3 (2.74e+2)−	5.23e+3 (1.03e+3)−	1.32e+3 (7.15e+1)
MaF5	7	9.21e+0 (5.02e-2)−	9.57e+0 (1.18e+0)−	8.91e+0 (2.85e+0)+	7.91e+0 (2.96e-1)+	9.25e+0 (3.05e-2)−	9.17e+0 (3.99e-1)
	10	8.70e+1 (1.38e+0)−	9.51e+1 (7.14e+0)−	5.47e+1 (1.33e+1)+	4.84e+1 (1.75e+0)+	8.80e+1 (1.71e+0)−	6.34e+1 (3.08e-2)
	15	2.39e+3 (2.78e+2)−	2.97e+3 (4.30e+2)−	1.56e+3 (5.86e+2)−	1.27e+3 (8.21e+1)+	2.26e+3 (2.27e+2)−	1.39e+3 (1.66e+2)
MaF6	7	3.01e-2 (3.43e-2)−	1.62e-1 (9.50e-2)−	7.42e-1 (6.59e-6)−	1.16e-2 (4.36e-2)−	9.87e-2 (2.23e-2)−	3.79e-3 (5.19e-5)
	10	7.43e+0 (2.41e+1)−	1.35e-1 (3.42e-2)−	7.37e-1 (1.74e-2)−	2.77e-1 (7.57e-2)−	2.21e-1 (1.12e-1)−	2.86e-3 (7.85e-7)
	15	8.91e+0 (9.65e+0)−	4.54e-1 (2.70e-1)−	7.09e-1 (4.55e-2)−	3.21e-1 (4.70e-2)−	3.61e+1 (3.49e+1)−	3.74e-3 (1.17e-6)
MaF7	7	6.03e-1 (5.53e-2)−	8.67e-1 (7.28e-2)−	1.28e+0 (1.62e-1)−	5.69e-1 (1.33e-2)≈	6.69e-1 (3.26e-2)−	5.69e-1 (1.82e-2)
	10	1.30e+0 (1.29e-1)−	1.90e+0 (3.98e-1)−	2.66e+0 (5.66e-1)−	9.55e-1 (1.82e-2)+	1.98e+0 (2.30e-2)−	9.75e-1 (1.52e-2)
	15	3.68e+0 (6.85e-1)−	2.70e+0 (5.10e-1)−	1.30e+1 (5.88e+0)−	1.97e+0 (1.10e-1)−	2.43e+1 (2.17e+1)−	1.80e+0 (2.41e-2)
WFG1	7	1.02e+0 (7.94e-2)−	9.53e-1 (1.06e-1)−	1.83e+0 (4.65e-1)−	7.68e-1 (4.58e-2)+	7.89e-1 (4.01e-2)+	8.21e-1 (5.80e-2)
	10	1.49e+0 (1.02e-1)−	1.52e+0 (1.39e-1)−	2.47e+0 (4.46e-1)−	1.13e+0 (6.54e-2)−	1.37e+0 (6.45e-2)−	1.22e+0 (6.86e-2)
	15	2.21e+0 (2.16e-1)−	1.98e+0 (1.35e-1)−	2.95e+0 (4.09e-1)−	1.80e+0 (7.94e-2)−	1.81e+0 (1.58e-1)−	1.79e+0 (1.21e-1)
WFG2	7	2.48e+0 (7.44e-1)−	5.40e+0 (1.02e+0)−	1.37e+0 (1.37e-1)+	2.22e+0 (2.62e-1)−	2.00e+0 (2.02e-1)+	2.08e+0 (2.14e-1)
	10	5.18e+0 (1.60e+0)−	7.54e+0 (2.12e+0)−	2.49e+0 (3.70e-1)+	2.87e+0 (2.69e-1)−	2.17e+0 (7.15e-1)+	2.41e+0 (1.82e-1)
	15	1.31e+1 (1.10e+0)−	1.85e+1 (4.84e+0)−	5.58e+0 (1.01e+0)−	1.02e+0 (3.66e-1)−	1.84e-1 (2.13e-1)−	5.11e-3 (1.52e-3)
WFG3	7	1.33e+0 (2.16e-1)−	1.52e+0 (2.54e-1)−	2.17e+0 (3.79e-1)−	1.08e+0 (1.62e-1)−	1.41e+0 (1.04e-1)−	2.55e-1 (1.13e-1)
	10	1.73e+0 (7.70e-1)−	4.15e+0 (6.89e-1)−	3.30e+0 (6.46e-1)−	1.83e+0 (1.99e-1)−	1.80e+0 (3.57e-2)−	5.15e-1 (2.88e-1)
	15	3.79e+0 (1.20e+0)−	8.07e+0 (2.04e+0)−	4.62e+0 (1.36e+0)−	3.65e+0 (1.81e-1)−	4.06e+0 (3.21e-1)−	1.14e+0 (6.99e-1)
WFG4	7	2.25e+0 (3.78e-2)+	2.22e+0 (6.07e-3)+	2.57e+0 (1.03e-1)+	2.27e+0 (1.84e-2)+	2.23e+0 (1.06e-3)+	2.64e+0 (2.63e-2)
	10	4.78e+0 (1.86e-1)+	4.59e+0 (6.08e-2)+	5.28e+0 (3.55e-1)+	4.19e+0 (2.80e-2)+	4.78e+0 (7.74e-3)+	4.82e+0 (3.60e-2)
	15	8.47e+0 (3.07e-1)−	8.87e+0 (1.30e-1)−	1.24e+1 (1.19e+0)−	7.43e+0 (7.94e-2)+	8.04e+0 (1.65e-2)+	8.05e+0 (7.10e-2)
WFG5	7	2.22e+0 (6.96e-3)−	2.21e+0 (4.79e-3)−	2.55e+0 (7.30e-2)−	2.26e+0 (1.52e-2)−	2.23e+0 (2.01e-4)−	2.19e+0 (1.07e-2)
	10	4.71e+0 (1.15e-2)+	4.59e+0 (6.86e-2)+	4.95e+0 (1.69e-1)−	4.18e+0 (2.84e-2)+	4.75e+0 (3.19e-3)+	4.78e+0 (3.36e-2)
	15	7.90e+0 (1.75e-1)+	8.80e+0 (1.13e-1)−	1.10e+1 (1.01e+0)−	7.18e+0 (5.79e-2)+	7.94e+0 (1.33e-2)+	7.95e+0 (6.43e-2)
WFG6	7	2.26e+0 (8.54e-3)+	2.24e+0 (2.91e-2)+	2.64e+0 (8.22e-2)−	2.29e+0 (2.20e-2)+	2.24e+0 (4.44e-3)+	2.63e+0 (2.56e-2)
	10	5.02e+0 (6.63e-1)−	4.43e+0 (9.06e-2)+	4.93e+0 (2.52e-1)−	4.25e+0 (3.68e-2)+	4.78e+0 (1.13e-2)+	4.82e+0 (3.78e-2)
	15	9.94e+0 (8.49e-1)−	9.23e+0 (3.47e-1)−	1.09e+1 (9.73e-1)−	7.23e+0 (5.58e-2)−	8.04e+0 (2.51e-2)−	7.19e+0 (4.64e-2)
WFG7	7	2.26e+0 (7.59e-3)−	2.21e+0 (7.28e-3)−	2.79e+0 (1.63e-1)−	2.26e+0 (1.93e-2)−	2.25e+0 (3.18e-3)−	2.20e+0 (8.51e-3)
	10	4.77e+0 (9.55e-2)−	4.57e+0 (3.67e-2)−	5.15e+0 (2.23e-1)−	4.17e+0 (2.11e-2)−	4.79e+0 (7.72e-3)−	4.05e+0 (2.12e-2)
	15	8.91e+0 (5.89e-1)−	7.72e+0 (5.34e-1)+	1.31e+1 (8.84e-1)−	7.21e+0 (4.84e-2)+	8.11e+0 (2.34e-2)−	7.98e+0 (4.55e-2)
WFG8	7	2.40e+0 (1.30e-1)−	2.41e+0 (3.92e-2)−	2.97e+0 (1.43e-1)−	2.43e+0 (2.72e-2)+	2.35e+0 (4.75e-2)+	2.67e+0 (4.56e-2)
	10	4.94e+0 (5.22e-1)−	4.36e+0 (6.93e-2)+	5.70e+0 (3.52e-1)+	4.45e+0 (3.86e-2)+	4.79e+0 (1.53e-2)−	4.74e+0 (5.49e-2)
	15	9.44e+0 (7.76e-1)−	8.91e+0 (3.76e-1)−	1.25e+1 (8.96e-1)−	7.37e+0 (2.50e-1)+	8.55e+0 (4.40e-2)−	8.15e+0 (1.21e-1)
WFG9	7	2.23e+0 (2.32e-2)+	2.20e+0 (7.97e-3)+	2.76e+0 (8.74e-2)−	2.23e+0 (1.92e-2)+	2.24e+0 (1.16e-2)+	2.60e+0 (2.31e-2)
	10	4.51e+0 (5.86e-2)+	4.48e+0 (6.77e-2)+	5.20e+0 (1.89e-1)−	4.13e+0 (2.47e-2)+	4.71e+0 (9.00e-3)+	4.72e+0 (7.25e-2)
	15	8.01e+0 (2.24e-1)−	7.69e+0 (2.72e-1)−	1.063e+1 (4.84e-1)−	6.93e+0 (5.23e-2)+	8.23e+0 (7.81e-2)−	7.68e+0 (1.05e-1)

of the output solution set obtained by *RVEA* are very poor. The complicated PF shape of MaF1 also weakens the convergence and diversity of *MaOEA-R&D* and *SPEA/R*, which is illustrated in Fig. 2(c) and (e). Fig. 2(d) shows that *VaEA* has better convergence and diversity than the other four comparison algorithms. By comparing Fig. 2(e) with Fig. 2(f), we can note that the distribution of the solution set obtained by the proposed TSEA is much better than *VaEA*. This also can explain why the HV and IGD values obtained by TSEA are much better than that obtained by the other five algorithms on the 10-objective MaF1, which are illustrated in the second row of Tables I and II.

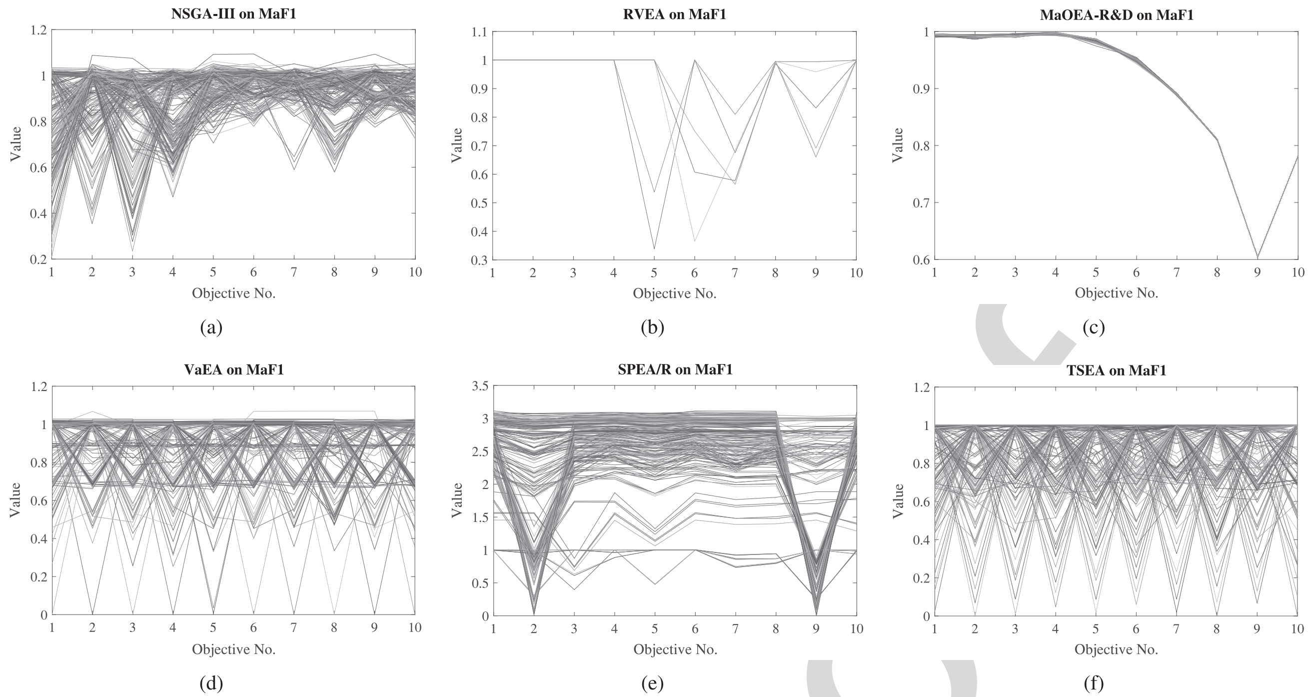

Fig. 2. Solution set obtained by each algorithm on the 10-objective MaF1, shown by parallel coordinates.

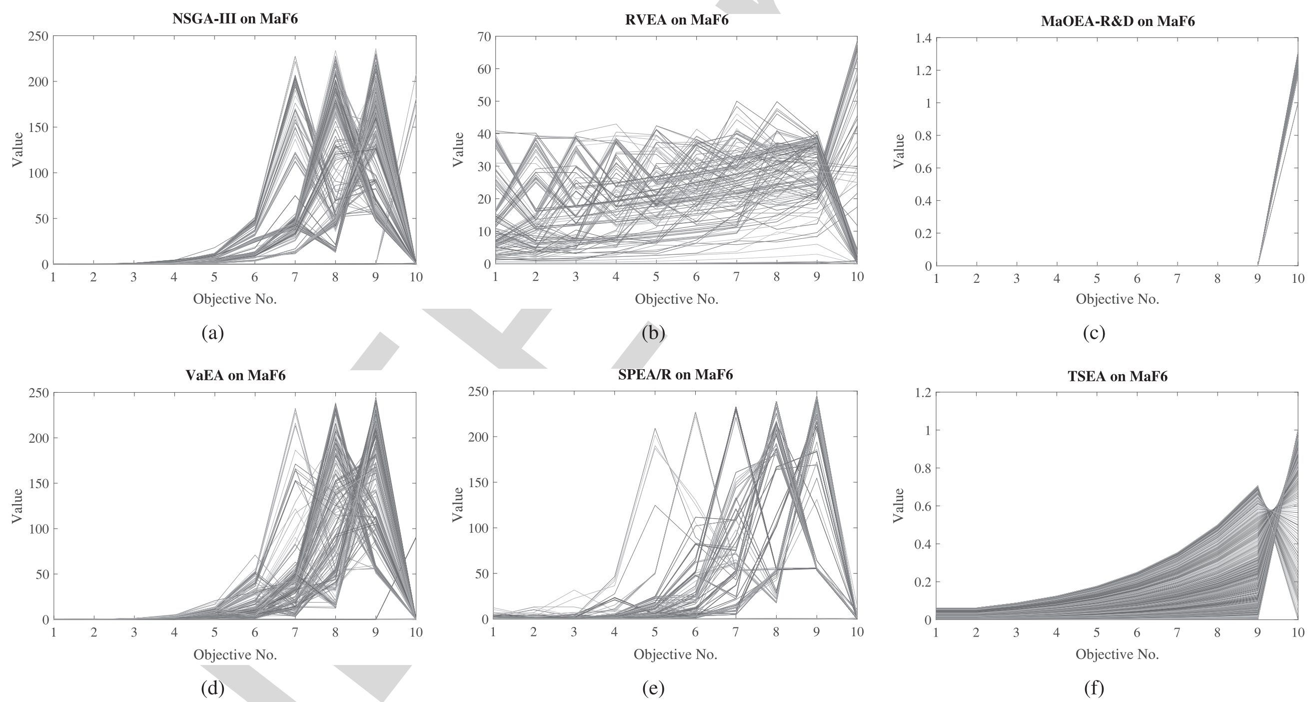

Fig. 3. Solution set obtained by each algorithm on the 10-objective MaF6, shown by parallel coordinates.

Since benchmark function MaF6 is a representative of MOPs with degenerate PFs, we also show the distribution of populations obtained by the six algorithms. As illustrated in Fig. 3, the convergence of *NSGA-III*, *RVEA*, *VaEA*, and *SPEA/R* is outperformed by the proposed TSEA. The algorithm *MaOEA-R&D* is similar to TSEA with respect to convergence, but the diversity of the proposed TSEA is better than that of *MaOEA-R&D*. This comparison results demonstrate the superiority of TSEA in solving MaOPs with disconnected PFs. In addition, the benchmark function WFG3 has also degenerate PF. For the test instance, i.e., 10-objective WFG3, it can be clearly observed that the proposed TSEA also outperforms the other five compared algorithms in terms of both convergence and diversity, which are illustrated in Fig. 4.

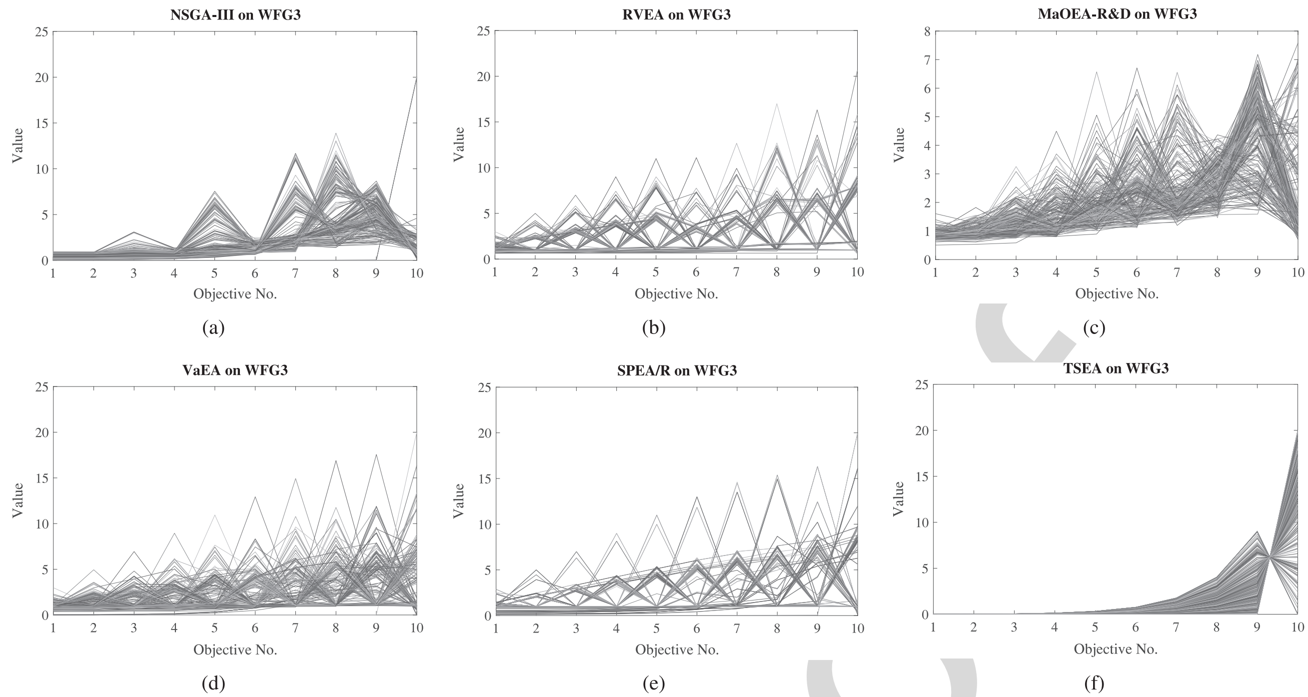

Fig. 4. Solution set obtained by each algorithm on the 10-objective WFG3, shown by parallel coordinates.

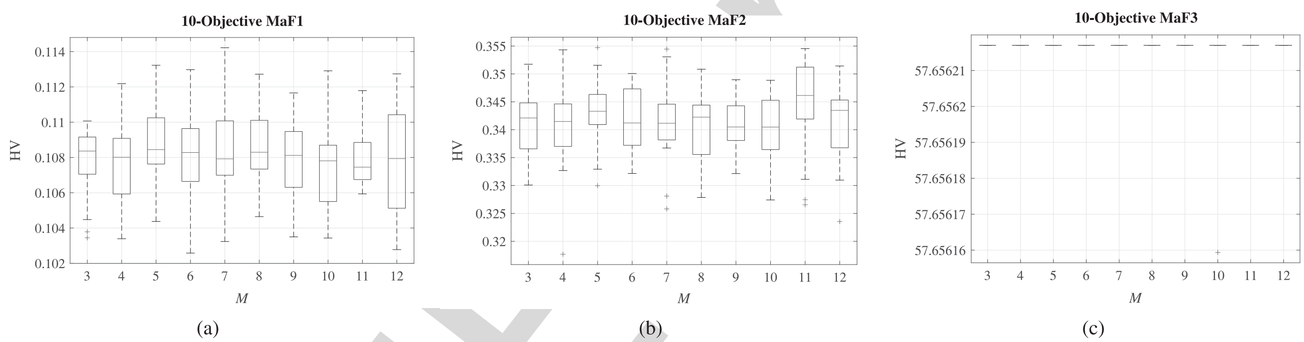

Fig. 5. Distributions of HV values obtained by TSEA over 30 runs by changing the parameter M.

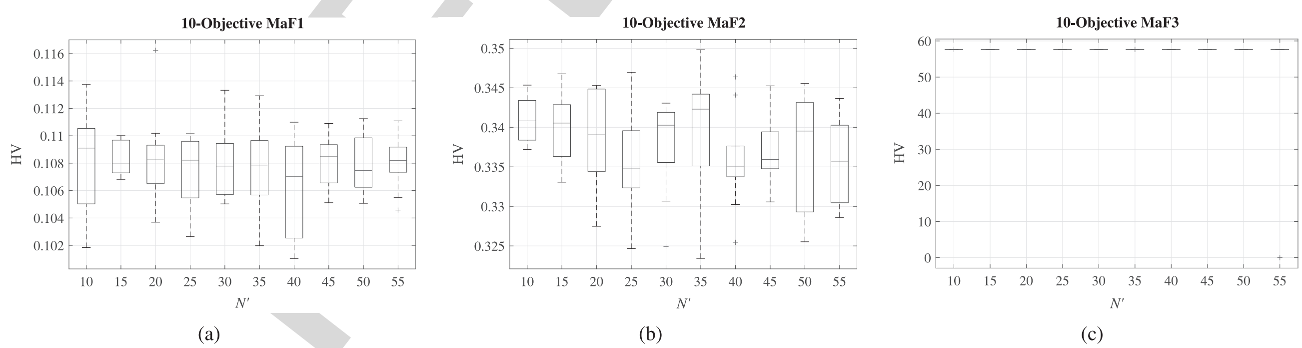

Fig. 6. Distributions of HV values obtained by TSEA over 30 runs by changing the parameter N'.

C. Sensitivity Analysis for Parameters M, N', and Δ

In the proposed TSEA, there are three tunable parameters: 1) the number of subpopulations M; 2) the size of a subpopulation N'; and 3) the convergence threshold Δ. To analyze the impact of these three parameters, in each experiment, we change the value of one parameter and fix the other two parameters. Besides, each experiment is repeated 30 times, and the box plots of the three parameters on 10-objective MaF1–MaF3 are illustrated in Figs. 5–7.

To test the impact of parameter M, it is varied from 3 to 12 with an increment of 1, while N' and Δ are fixed

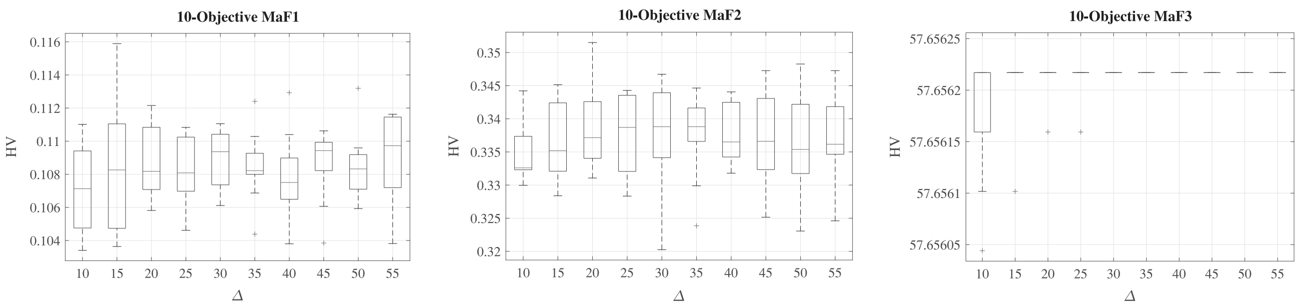

(a) (b) (c)

Fig. 7. Distributions of HV values obtained by TSEA over 30 runs by changing the parameter Δ.

to 20 and 1e-10, respectively. Fig. 5 shows that the HV values obtained by TSEA on the three test instances basically remain unchanged when varying parameter M. This result demonstrates that the parameter M has little impact on the performance of the proposed TSEA when it is between 3 and 12. A similar observation can be found in Fig. 6. When the size of each subpopulation is changed from 10 to 55, the HV values of TSEA on 10-objective MaF1, MaF2, and MaF3 are stable around 0.108, 0.336, and 57.656, respectively. This result illustrates that the parameter N' also has little impact on the performance of TSEA.

For parameter Δ, we change it from 1e-3 to 1e-12 to analyze its impact on the performance of the proposed TSEA. As shown in Fig. 7, we can see that the mean HV values obtained by TSEA on 10-objective MaF1 and MaF2 increase slightly with the decrease of parameter Δ. This can be attributed to the fact that lower Δ enables TSEA to push the subpopulations at the first stage closer to the PF, which is more helpful for balancing the convergence and diversity at the second stage. On the basis of the above analysis, we recommend the parameter Δ be lower than 1e–10 for the proposed TSEA.

V. CONCLUSION

This paper has proposed to solve MaOPs by partitioning the whole evolutionary search process into two stages, where the first stage focuses on the population convergence, and the second stage strives to improve the population diversity. To avoid the negative influence of the complicated PF shapes and accelerating the convergence speed of the population, all subpopulations at first stage only focuses on the convergence, and different weight vectors were used to guide them converge to different areas of PF. Then, to improve the population diversity, an environmental selection strategy has also proposed for the second stage to select the candidate solutions with promising diversity. Using such a multistage evolutionary search strategy, the proposed TSEA demonstrated ascendant performance over the five representative algorithms.

With the increase of the number of decision variables, the search spaces of optimization problems are exponentially exploded, which seriously challenge the performance of evolutionary algorithms. Thus, solving MaOPs having thousands of decision variables is an interesting direction.

REFERENCES

[1] X.-L. Zheng and L. Wang, "A collaborative multiobjective fruit fly optimization algorithm for the resource constrained unrelated parallel machine green scheduling problem," *IEEE Trans. Syst., Man, Cybern., Syst.*, vol. 48, no. 5, pp. 790–800, May 2018.

[2] R. Cheng, T. Rodemann, M. Fischer, M. Olhofer, and Y. Jin, "Evolutionary many-objective optimization of hybrid electric vehicle control: From general optimization to preference articulation," *IEEE Trans. Emerg. Topics Comput. Intell.*, vol. 1, no. 2, pp. 97–111, Apr. 2017.

[3] H. Chen, X. Zhu, G. Liu, and W. Pedrycz, "Uncertainty-aware online scheduling for real-time workflows in cloud service environment," *IEEE Trans. Services Comput.*, to be published. doi: 10.1109/TSC.2018.2866421.

[4] Z. Wang, Y.-S. Ong, J. Sun, A. Gupta, and Q. Zhang, "A generator for multiobjective test problems with difficult-to-approximate Pareto front boundaries," *IEEE Trans. Evol. Comput.*, to be published. doi: 10.1109/TEVC.2018.2872453.

[5] Y. R. Naidu and A. K. Ojha, "Solving multiobjective optimization problems using hybrid cooperative invasive weed optimization with multiple populations," *IEEE Trans. Syst., Man, Cybern., Syst.*, vol. 48, no. 6, pp. 821–832, Jun. 2018.

[6] M. Farina and P. Amato, "On the optimal solution definition for many-criteria optimization problems," in *Proc. IEEE Annu. Meeting North Amer. Fuzzy Inf. Process. Soc.*, 2002, pp. 233–238.

[7] L. Zhen, "A bi-objective model on multiperiod green supply chain network design," *IEEE Trans. Syst., Man, Cybern., Syst.*, to be published. doi: 10.1109/TSMC.2017.2690444.

[8] Z. Wang, Y.-S. Ong, and H. Ishibuchi, "On scalable multiobjective test problems with hardly-dominated boundaries," *IEEE Trans. Evol. Comput.*, vol. 23, no. 2, pp. 217–231, Apr. 2019.

[9] R. Wang, R. C. Purshouse, and P. J. Fleming, "Preference-inspired co-evolutionary algorithms using weight vectors," *Eur. J. Oper. Res.*, vol. 243, no. 2, pp. 423–441, 2015.

[10] R. Cheng, Y. Jin, M. Olhofer, and B. Sendhoff, "A reference vector guided evolutionary algorithm for many-objective optimization," *IEEE Trans. Evol. Comput.*, vol. 20, no. 5, pp. 773–791, Oct. 2016.

[11] H. Chen, R. Cheng, J. Wen, H. Li, and J. Weng, "Solving large-scale many-objective optimization problems by covariance matrix adaptation evolution strategy with scalable small subpopulations," *Inf. Sci.*, Oct. 2018. doi: 10.1016/j.ins.2018.10.007.

[12] B. Li, J. Li, K. Tang, and X. Yao, "Many-objective evolutionary algorithms: A survey," *ACM Comput. Surveys*, vol. 48, no. 1, pp. 1–35, 2015.

[13] A. Trivedi, D. Srinivasan, K. Sanyal, and A. Ghosh, "A survey of multiobjective evolutionary algorithms based on decomposition," *IEEE Trans. Evol. Comput.*, vol. 21, no. 3, pp. 440–462, Jun. 2017.

[14] K. Deb, A. Pratap, S. Agarwal, and T. Meyarivan, "A fast and elitist multiobjective genetic algorithm: NSGA-II," *IEEE Trans. Evol. Comput.*, vol. 6, no. 2, pp. 182–197, Apr. 2002.

[15] C. A. Coello Coello, G. T. Pulido, and M. S. Lechuga, "Handling multiple objectives with particle swarm optimization," *IEEE Trans. Evol. Comput.*, vol. 8, no. 3, pp. 256–279, Jun. 2004.

[16] J. Bader and E. Zitzler, "HypE: An algorithm for fast hypervolume-based many-objective optimization," *Evol. Comput.*, vol. 19, no. 1, pp. 45–76, Mar. 2011.

[17] Y. Tian, R. Cheng, X. Zhang, F. Cheng, and Y. Jin, "An indicator based multi-objective evolutionary algorithm with reference point adaptation for better versatility," *IEEE Trans. Evol. Comput.*, vol. 22, no. 4, pp. 609–622, Aug. 2018.

[18] M. Li, S. Yang, and X. Liu, "Bi-goal evolution for many-objective optimization problems," *Artif. Intell.*, vol. 228, pp. 45–65, Nov. 2015.

[19] Q. Zhang and H. Li, "MOEA/D: A multiobjective evolutionary algorithm based on decomposition," *IEEE Trans. Evol. Comput.*, vol. 11, no. 6, pp. 712–731, Dec. 2007.

[20] H.-L. Liu, F. Gu, and Q. Zhang, "Decomposition of a multiobjective optimization problem into a number of simple multiobjective subproblems," *IEEE Trans. Evol. Comput.*, vol. 18, no. 3, pp. 450–455, Jun. 2014.

[21] Z. Wang, Q. Zhang, A. Zhou, M. Gong, and L. Jiao, "Adaptive replacement strategies for MOEA/D," *IEEE Trans. Cybern.*, vol. 46, no. 2, pp. 474–486, Feb. 2016.

[22] K. Deb and H. Jain, "An evolutionary many-objective optimization algorithm using reference-point-based nondominated sorting approach, part I: Solving problems with box constraints," *IEEE Trans. Evol. Comput.*, vol. 18, no. 4, pp. 577–601, Aug. 2014.

[23] H. Ishibuchi, N. Akedo, and Y. Nojima, "Behavior of multiobjective evolutionary algorithms on many-objective knapsack problems," *IEEE Trans. Evol. Comput.*, vol. 19, no. 2, pp. 264–283, Apr. 2015.

[24] R. C. Purshouse and P. J. Fleming, "On the evolutionary optimization of many conflicting objectives," *IEEE Trans. Evol. Comput.*, vol. 11, no. 6, pp. 770–784, Dec. 2007.

[25] Y. Xiang, Y. Zhou, M. Li, and Z. Chen, "A vector angle-based evolutionary algorithm for unconstrained many-objective optimization," *IEEE Trans. Evol. Comput.*, vol. 21, no. 1, pp. 131–152, Feb. 2017.

[26] H. Ishibuchi, Y. Setoguchi, H. Masuda, and Y. Nojima, "Performance of decomposition-based many-objective algorithms strongly depends on Pareto front shapes," *IEEE Trans. Evol. Comput.*, vol. 21, no. 2, pp. 169–190, Apr. 2017.

[27] S. Jiang and S. Yang, "A strength Pareto evolutionary algorithm based on reference direction for multi-objective and many-objective optimization," *IEEE Trans. Evol. Comput.*, vol. 21, no. 3, pp. 329–346, Jun. 2017.

[28] A. Zhou, B.-Y. Qu, H. Li, S.-Z. Zhao, P. N. Suganthan, and Q. Zhang, "Multiobjective evolutionary algorithms: A survey of the state-of-the-art," *Swarm Evol. Comput.*, vol. 1, no. 1, pp. 32–49, 2011.

[29] D. W. Corne, N. R. Jerram, J. D. Knowles, and M. J. Oates, "PESA-II: Region-based selection in evolutionary multiobjective optimization," in *Genetic and Evolutionary Computation*, Morgan Kaufmann, 2001, pp. 283–290. AQ4

[30] E. Zitzler, M. Laumanns, and L. Thiele, "SPEA2: Improving the strength Pareto evolutionary algorithm," in *Proc. Evol. Methods Design Optim. Control Appl. Ind. Problems*, 2002, pp. 95–100.

[31] C.-H. Chen and J.-H. Chou, "Multiobjective optimization of airline crew roster recovery problems under disruption conditions," *IEEE Trans. Syst., Man, Cybern., Syst.*, vol. 47, no. 1, pp. 133–144, Jan. 2017.

[32] Y. Hou, N. Wu, M. Zhou, and Z. Li, "Pareto-optimization for scheduling of crude oil operations in refinery via genetic algorithm," *IEEE Trans. Syst., Man, Cybern., Syst.*, vol. 47, no. 3, pp. 517–530, Mar. 2017.

[33] Y. Yuan, H. Xu, B. Wang, and X. Yao, "A new dominance relation-based evolutionary algorithm for many-objective optimization," *IEEE Trans. Evol. Comput.*, vol. 20, no. 1, pp. 16–37, Feb. 2016.

[34] H. Wang and X. Yao, "Corner sort for Pareto-based many-objective optimization," *IEEE Trans. Cybern.*, vol. 44, no. 1, pp. 92–102, Jan. 2014.

[35] S. Yang, M. Li, X. Liu, and J. Zheng, "A grid-based evolutionary algorithm for many-objective optimization," *IEEE Trans. Evol. Comput.*, vol. 17, no. 5, pp. 721–736, Oct. 2013.

[36] Z. He, G. G. Yen, and J. Zhang, "Fuzzy-based Pareto optimality for many-objective evolutionary algorithms," *IEEE Trans. Evol. Comput.*, vol. 18, no. 2, pp. 269–285, Apr. 2014.

[37] H. Chen, Y. Tian, W. Pedrycz, G. Wu, R. Wang, and L. Wang, "Hyperplane assisted evolutionary algorithm for many-objective optimization problems," *IEEE Trans. Cybern.*, to be published. doi: 10.1109/TCYB.2019.2899225.

[38] E. Zitzler and S. Künzli, "Indicator-based selection in multiobjective search," in *Proc. Parallel Problem Solving Nat.*, 2004, pp. 832–842.

[39] N. Beume, B. Naujoks, and M. Emmerich, "SMS-EMOA: Multiobjective selection based on dominated hypervolume," *Eur. J. Oper. Res.*, vol. 181, no. 3, pp. 1653–1669, 2007.

[40] K. Bringmann, T. Friedrich, C. Igel, and T. Voß, "Speeding up many-objective optimization by Monte Carlo approximations," *Artif. Intell.*, vol. 204, pp. 22–29, Nov. 2013.

[41] C. Zhou, G. Dai, M. Wang, and X. Li, "Indicator and reference points co-guided evolutionary algorithm for many-objective optimization problems," *Knowl. Based Syst.*, vol. 140, pp. 50–63, Jan. 2018.

[42] R. Wang, R. C. Purshouse, and P. J. Fleming, "Preference-inspired coevolutionary algorithms for many-objective optimization," *IEEE Trans. Evol. Comput.*, vol. 17, no. 4, pp. 474–494, Aug. 2013.

[43] K. Li, K. Deb, Q. Zhang, and S. Kwong, "An evolutionary many-objective optimization algorithm based on dominance and decomposition," *IEEE Trans. Evol. Comput.*, vol. 19, no. 5, pp. 694–716, Oct. 2015.

[44] Y. Qi, X. Ma, F. Liu, L. Jiao, J. Sun, and J. Wu, "MOEA/D with adaptive weight adjustment," *Evol. Comput.*, vol. 22, no. 2, pp. 231–264, 2014.

[45] R. Wang, Q. Zhang, and T. Zhang, "Decomposition-based algorithms using Pareto adaptive scalarizing methods," *IEEE Trans. Evol. Comput.*, vol. 20, no. 6, pp. 821–837, Dec. 2016.

[46] X. Cai, Z. Yang, Z. Fan, and Q. Zhang, "Decomposition-based-sorting and angle-based-selection for evolutionary multiobjective and many-objective optimization," *IEEE Trans. Cybern.*, vol. 47, no. 9, pp. 2824–2837, Sep. 2017.

[47] X. Cai, Z. Mei, Z. Fan, and Q. Zhang, "A constrained decomposition approach with grids for evolutionary multiobjective optimization," *IEEE Trans. Evol. Comput.*, vol. 22, no. 4, pp. 564–577, Aug. 2018.

[48] M. Elarbi, S. Bechikh, A. Gupta, L. B. Said, and Y.-S. Ong, "A new decomposition-based NSGA-II for many-objective optimization," *IEEE Trans. Syst., Man, Cybern., Syst.*, vol. 48, no. 7, pp. 1191–1210, Jul. 2018.

[49] R. Wang, Z. Zhou, H. Ishibuchi, T. Liao, and T. Zhang, "Localized weighted sum method for many-objective optimization," *IEEE Trans. Evol. Comput.*, vol. 22, no. 1, pp. 3–18, Feb. 2018.

[50] H.-L. Liu, L. Chen, Q. Zhang, and K. Deb, "Adaptively allocating search effort in challenging many-objective optimization problems," *IEEE Trans. Evol. Comput.*, vol. 22, no. 3, pp. 433–448, Jun. 2018.

[51] H. Chen, G. Wu, W. Pedrycz, P. N. Suganthan, L. Xing, and X. Zhu, "An adaptive resource allocation strategy for objective space partition based multiobjective optimization," *IEEE Trans. Syst., Man, Cybern., Syst.*, to be published. doi: 10.1109/TSMC.2019.2898456.

[52] Q. Kang, X. Song, M. Zhou, and L. Li, "A collaborative resource allocation strategy for decomposition-based multiobjective evolutionary algorithms," *IEEE Trans. Syst., Man, Cybern., Syst.*, to be published. doi: 10.1109/TSMC.2018.2818175.

[53] X. Cai, H. Sun, C. Zhu, Z. Li, and Q. Zhang, "Locating the boundaries of Pareto fronts: A many-objective evolutionary algorithm based on corner solution search," *arXiv preprint arXiv:1806.02967*, 2018. AQ5

[54] W. Hu, G. G. Yen, and G. Luo, "Many-objective particle swarm optimization using two-stage strategy and parallel cell coordinate system," *IEEE Trans. Cybern.*, vol. 47, no. 6, pp. 1446–1459, Jun. 2017.

[55] Y. Sun, B. Xue, M. Zhang, and G. G. Yen, "A new two-stage evolutionary algorithm for many-objective optimization," *IEEE Trans. Evol. Comput.*, to be published. doi: 10.1109/TEVC.2018.2882166.

[56] Y. Liu, D. Gong, J. Sun, and Y. Jin, "A many-objective evolutionary algorithm using a one-by-one selection strategy," *IEEE Trans. Cybern.*, vol. 47, no. 9, pp. 2689–2702, Sep. 2017.

[57] S. Huband, P. Hingston, L. Barone, and L. While, "A review of multiobjective test problems and a scalable test problem toolkit," *IEEE Trans. Evol. Comput.*, vol. 10, no. 5, pp. 477–506, Oct. 2006.

[58] X. Ma *et al.*, "A multiobjective evolutionary algorithm based on decision variable analyses for multiobjective optimization problems with large-scale variables," *IEEE Trans. Evol. Comput.*, vol. 20, no. 2, pp. 275–298, Apr. 2016.

[59] Z. He and G. G. Yen, "Many-objective evolutionary algorithm: Objective space reduction and diversity improvement," *IEEE Trans. Evol. Comput.*, vol. 20, no. 1, pp. 145–160, Feb. 2016.

[60] R. Cheng *et al.*, "A benchmark test suite for evolutionary many-objective optimization," *Complex Intell. Syst.*, vol. 3, no. 1, pp. 67–81, 2017.

[61] E. Zitzler and L. Thiele, "Multiobjective evolutionary algorithms: A comparative case study and the strength Pareto approach," *IEEE Trans. Evol. Comput.*, vol. 3, no. 4, pp. 257–271, Nov. 1999.

[62] P. A. N. Bosman and D. Thierens, "The balance between proximity and diversity in multiobjective evolutionary algorithms," *IEEE Trans. Evol. Comput.*, vol. 7, no. 2, pp. 174–188, Apr. 2003.

AQ6

Huangke Chen received the B.S. degree in management science and engineering and the M.S. degree in operations research from the College of Information and System Management, National University of Defense Technology, Changsha, China, in 2012 and 2014, respectively, where he is currently pursuing the Ph.D. degree with the College of Systems Engineering.

He was a visiting Ph.D. student with the University of Alberta, Edmonton, AB, Canada, from 2017 to 2018. His current research interests include computational intelligence, multiobjective evolutionary algorithms, large-scale optimization, and task and workflow scheduling.

AQ7

Ran Cheng (M'16) received the B.Sc. degree from Northeastern University, Shenyang, China, in 2010, and the Ph.D. degree from the University of Surrey, Guildford, U.K., in 2016.

He is currently an Assistant Professor with the Department of Computer Science and Engineering, Southern University of Science and Technology, Shenzhen, China. His current research interests include evolutionary multiobjective optimization, model-based evolutionary algorithms, large-scale optimization, swarm intelligence, and deep learning.

Dr. Cheng was a recipient of the 2018 IEEE TRANSACTIONS ON EVOLUTIONARY COMPUTATION Outstanding Paper Award, the 2019 IEEE Computational Intelligence Society Outstanding Ph.D. Dissertation Award, and the 2020 *IEEE Computational Intelligence Magazine* Outstanding Paper Award. He is the Founding Chair of IEEE Symposium on Model-Based Evolutionary Algorithms.

Witold Pedrycz (F'99) received the M.Sc., Ph.D., and D.Sc. degrees in computer science from the Silesian University of Technology, Gliwice, Poland.

He is a Professor and the Canada Research Chair of CRC-Computational Intelligence with the Department of Electrical and Computer Engineering, University of Alberta, Edmonton, AB, Canada, also with the Department of Electrical and Computer Engineering, Faculty of Engineering, King Abdulaziz University, Jeddah, Saudi Arabia, and also with the Systems Research Institute, Polish Academy of Sciences, Warsaw, Poland. His current research interests include computational intelligence, fuzzy modeling and granular computing, knowledge discovery and data mining, fuzzy control, pattern recognition, knowledge-based neural networks, relational computing, and software engineering. He has published numerous papers in the above areas.

Prof. Pedrycz is the Editor-in-Chief of *Information Sciences* and serves as an Associate Editor for the IEEE TRANSACTIONS ON SYSTEMS, MAN, AND CYBERNETICS: SYSTEMS and IEEE TRANSACTIONS ON FUZZY SYSTEMS. He is also on the editorial board of other international journals.

Yaochu Jin (M'98–SM'02–F'16) received the B.Sc., M.Sc., and Ph.D. degrees from Zhejiang University, Hangzhou, China, in 1988, 1991, and 1996, respectively, and the Dr.-Ing. degree from Ruhr University Bochum, Bochum, Germany, in 2001.

He is a Professor of Computational Intelligence with the Department of Computer Science, University of Surrey, Guildford, U.K., where he heads the Nature Inspired Computing and Engineering Group. He is also a Finland Distinguished Professor funded by the Finnish Agency for Innovation (Tekes) and a Changjiang Distinguished Visiting Professor appointed by the Ministry of Education, Beijing, China. He has coauthored over 200 peer-reviewed journal and conference papers and been granted eight patents on evolutionary optimization. His current research is funded by EC FP7, U.K. EPSRC, and industry. He has delivered over 20 invited keynote speeches at international conferences. His science-driven research interests include interdisciplinary areas that bridge the gap between computational intelligence, computational neuroscience, and computational systems biology. He is also particularly interested in nature-inspired and real-world-driven problem solving.

Prof. Jin was a recipient of the Best Paper Award of the 2010 IEEE Symposium on Computational Intelligence in Bioinformatics and Computational Biology and the 2014 and 2017 *IEEE Computational Intelligence Magazine* Outstanding Paper Award. He is the Editor-in-Chief of the IEEE TRANSACTIONS ON COGNITIVE AND DEVELOPMENTAL SYSTEMS and *Complex and Intelligent Systems*. He is also an Associate Editor or an Editorial Board Member of the IEEE TRANSACTIONS ON EVOLUTIONARY COMPUTATION, IEEE TRANSACTIONS ON CYBERNETICS, IEEE TRANSACTIONS ON NANOBIOSCIENCE, *Evolutionary Computation*, *BioSystems*, *Soft Computing*, and *Natural Computing*. He is an IEEE Distinguished Lecturer from 2013 to 2015 and from 2017 to 2019, and was the Vice President for Technical Activities of the IEEE Computational Intelligence Society from 2014 to 2015.